L-383

NATIONAL ADVISORY COMMITTEE FOR AERONAUTICS

WARTIME REPORT

ORIGINALLY ISSUED
January 1943 as
Advance Restricted Report

FLIGHT INVESTIGATION OF NACA D_S COWLINGS ON THE XP-42 AIRPLANE. I - HIGH-INLET-VELOCITY COWLING WITH PROPELLER CUFFS TESTED IN HIGH-SPEED LEVEL FLIGHT

By F. J. Bailey, Jr., and J. Ford Johnston

Langley Memorial Aeronautical Laboratory
Langley Field, Va.

JPL LIBRARY
CALIFORNIA INSTITUTE OF TECHNOLOGY

NACA

WASHINGTON

NACA WARTIME REPORTS are reprints of papers originally issued to provide rapid distribution of advance research results to an authorized group requiring them for the war effort. They were previously held under a security status but are now unclassified. Some of these reports were not technically edited. All have been reproduced without change in order to expedite general distribution.

L-383

NATIONAL ADVISORY COMMITTEE FOR AERONAUTICS

ADVANCE RESTRICTED REPORT

FLIGHT INVESTIGATION OF NACA D_S COWLINGS ON THE XP-42 AIRPLANE. I - HIGH-INLET-VELOCITY COWLING WITH PROPELLER CUFFS TESTED IN HIGH-SPEED LEVEL FLIGHT

By F. J. Bailey, Jr., and J. Ford Johnston

SUMMARY

Results are presented of a series of flight tests of the maximum speed and cooling characteristics in full-throttle level flight of the XP-42 airplane equipped with a short-nose high-inlet-velocity cowling. This cowling is one of a series being tested in an effort to improve the performance and cooling characteristics of air-cooled engine installations.

The results of the tests indicated a maximum speed of 336 miles per hour at 960 horsepower at 15,000 feet.

Pressure measurements in the entrances to the cylinder baffles showed a fairly uniform distribution of pressure around the engine at similar points of measurement on individual cylinders but indicated that cooling-air pressures varied considerably for different points of measurement on the same cylinder. The variation was probably due to the velocity head of the entering cooling-air jet. Static pressure behind the engine was uniform.

Front pressures on the engine averaged 80 percent and rear pressures 39 percent of free-stream impact pressure. The resulting pressure drop of 15 inches of water at full throttle at 15,000 feet cooled the cylinder heads adequately; maximum cylinder base temperatures, however, exceeded the specified limits when corrected to Army summer conditions.

Pressure measurements in the carburetor and oil-cooler ducts showed rams of slightly over 100 percent of free-stream impact pressure. Air-flow measurements in the car-

buretor duct and in the annular entrance to the engine compartment showed that the volume flows of induction and cooling air were approximately constant at full throttle over a range of altitudes near the critical altitude and were, respectively, 2960 and 19,900 cubic feet of free air per minute.

INTRODUCTION

The National Advisory Committee for Aeronautics is investigating means of modifying the conventional NACA radial engine cowling to meet the demands imposed by the latest designs of military airplanes. Tests in a number of the wind tunnels have been directed toward improving the cowling in the following respects:

1. Greater stability of the air flow within the cowling, particularly at angles of attack corresponding to the climb condition, to provide a uniform cooling-air pressure in front of the engine

2. Reduction of energy losses in the cooling air in front of the engine by the use of an efficient diffuser between the inlet and the front face of engine

3. Adequate ground cooling characteristics

4. Improvement in the external shape to reduce drag and to increase the critical speed of the cowling

The NACA D-series cowlings have been developed to meet these requirements. The D cowlings are characterized by the use of a cowling inner liner and of an afterbody behind the spinner. These units form an annular entrance followed by a diffuser section made up of the afterbody and inner liner. Investigations such as reported in references 1 and 2 have indicated desirable ranges of cooling-air inlet velocities, diffuser proportions, and external contours.

In order to expedite incorporation of these new features in projected designs for military aircraft, the NACA is conducting flight tests of the Curtiss XP-42 airplane fitted with several engine installations utilizing the latest developments of the NACA cowling and individual cylinder jet exhaust stacks (reference 3).

The XP-42 airplane is powered by a Pratt & Whitney 1830-31 engine. As originally furnished with the airplane, this engine carried an extension shaft that placed the propeller 30 inches ahead of the normal position. The first of the cowlings included in the series of tests was designed for this long-nose engine and represented a complete redesign of the cowling furnished with the airplane. The development of this cowling in the full-scale wind tunnel is described in reference 2 and the flight-test results are presented in reference 4.

The present report is the first of a series of reports on the short-nose (D_S) cowlings and contains the results of tests in the high-speed level-flight condition of the high-inlet-velocity cowling, which was designed for the short-nose Pratt & Whitney 1830 engine. This cowling was tested on the XP-42 airplane by replacing the nose-extension shaft of the 1830-31 engine with a shaft of standard size.

For convenience, test numbers have been assigned each cowling arrangement and flight condition. Tests 1 and 2 were the high-speed and climb tests of the long-nose cowling and test 3 is the investigation on the short-nose cowling reported herein. Further identification has been given by prefixing this test number to the number for a particular flight, which was arbitrarily assigned. For example, flight 3-6 indicates flight 6 in which the airplane was in test condition 3.

It was necessary to defer the final part of the tests of this cowling, involving determination of its cooling characteristics in climb, until the scheduled high-speed tests of other arrangements had been completed and the inadequate cowl flap installation could be modified as in reference 4.

The design of the cowling and engine installation was a project of the Air-Cooled Engine-Installation Group stationed at the Laboratory. The members of the group associated with this project included Mr. Howard S. Ditsch, of the Curtiss Wright Corporation; Mr. Peter Torraco, of the Republic Aviation Corporation; Mr. William S. Richards, of the Wright Aeronautical Corporation; and Mr. James R. Thompson, of Pratt & Whitney Aircraft. The Materiel Command, Army Air Forces sponsored the investigation and supplied the XP-42 airplane. The Airplane Division of the Curtiss-Wright Corporation handled the construction as

well as the structural and detail design of the cowling, and supplied personnel to assist in the servicing and maintenance of the airplane and cowling during the tests. Pratt & Whitney Aircraft prepared the engine and torque meter for the tests and assisted in the operation and servicing of the engine. The propeller, cuffs, and spinner were supplied by the Propeller Division of the Curtiss-Wright Corporation.

This report was originally issued as a memorandum report for the Army Air Corps.

XP-42 AIRPLANE WITH SHORT-NOSE COWLING

The XP-42 airplane is identical with the P-36 airplane except for the fuselage fairing behind the cowling and the installation of its Pratt & Whitney 1830 engine with its higher critical altitude rating. The power rating of the engine is as follows:

	Brake horsepower	Engine speed (rpm)	Altitude (ft)
Take-off	1050	2550	0
Normal rating	1000	2300	8,500
Normal rating	1000	2450	11,500
Military rating	1000	2700	14,500

The engine has a single-stage blower with an impeller-drive ratio of 8.47:1 and a propeller-drive ratio of 9:16. The engine-cylinder baffles were reworked to minimize the leakage of air between adjoining baffles and to direct the cooling air on the cylinders in an efficient manner.

The 10-inch-diameter oil cooler furnished with the engine was replaced by an 11-inch U.A.P. cooler with the same core depth of 9 inches. Individual jet exhaust stacks were used in place of the standard collector ring. These stacks are made of 0.049-inch stainless-steel tubing of $2\frac{3}{8}$-inch outside diameter. The ends of the stacks were flattened to reduce the internal area from 4.05 to 2.98 square inches.

L-383

The engine cowling and propeller cuffs were fabricated by the Curtiss-Wright Corporation and are shown in figures 1 to 6.

The fuselage side panels reported in references 1 and 2 were used to improve the fairing of the cowling into the fuselage. The airplane, as prepared for the tests, weighed about 6000 pounds with 175-pound pilot and full tanks. It retained the standard aerial, but had no provisions for guns.

TEST APPARATUS

The installation of test equipment was designed to give as nearly as possible a continuous record of the pertinent data, with the exception of air-flow measurements, throughout each flight. Continuous records were taken of airspeed, altitude, manifold pressure, engine speed and torque, and temperatures. Air flows were measured by recording instruments during the particular flight conditions under investigation.

Free-stream impact pressure was measured by an NACA airspeed recorder connected to an airspeed boom on the right wing tip (fig. 7). The boom carried a fixed static head about one chord length ahead of the leading edge of the wing and a special shielded impact head halfway between the static head and the leading edge of the wing. The static head was calibrated in flight by flying at a known geometric height at several airspeeds with a sensitive altimeter (fig. 8) connected to the static head. The shielded impact head is accurate at all angles of attack encountered in steady flight.

Atmospheric pressure was measured by an NACA recording altimeter vented to the compartment behind the cockpit in which the recording instruments were installed. Pressure data so acquired were corrected for the measured difference between the compartment pressure and true static pressure.

In the same instrument was incorporated another cell that recorded absolute manifold pressure at the supercharger blower rim.

The pressure from a Pratt & Whitney oil-pressure torque meter installed in the nose of the engine was trans-

mitted both to a gage in the pilot's cockpit and to an NACA pressure recorder having a range of 400 pounds per square inch. This installation permitted both visual and recorded indications of the torque delivered to the propeller. This record, in conjunction with the engine-speed record, permitted calculation of the brake horsepower delivered to the propeller at any time during the flight.

Engine speed was recorded by means of a revolution counter tood off the tachometer drive. At every 200th revolution of the engine, a contact was made that operated a solenoid and made a mark on the airspeed film. Since a chronometric timer was also used to mark the film every 3 seconds, the time for 200 revolutions could be calculated from the relative distances along the film of engine speed and timer marks.

All temperature records were made by means of thermocouples connected through two 34-position rotating switches to a two-cell recording galvanometer. The cold junctions of all thermocouples were placed in pans surrounded by an ice-and-water bath to keep them at constant temperature. The leads to the cold-junction box are shown in figure 9. The box containing the ice-and-water bath is concealed by the felt wrapping used to insulate the bath from the cockpit temperatures. The switch speed was such that each temperature was recorded about once every 45 seconds.

All cylinder-head and barrel temperatures were measured, the heads by means of gasket-type thermocouples under the rear spark plugs, and the barrels by means of thermocouples peened into the flanges at the rear center line. Other temperature recordings included:

Intake mixture at intake ports of cylinders 5 and 10

Front and rear spark-plug elbows of cylinders 1, 7, and 11

Right and left magnetos

Fuel on suction and pressure sides of pump and in carburetor float chamber

Mixture at supercharger blower rim

L-383

Oil out

Oil-in line

Free air (under left wing outside slipstream, see figs. 10 and 11)

Air just ahead of screen in carburetor scoop

Air at entrance to engine compartment

Engine cooling air ahead of cylinder 1 and between cylinders 2 and 14

Engine cooling air 2 inches behind cylinder 1 and three fin spaces above bottom of head

Air at exit from oil cooler

Accessory compartment

Pilot's cockpit

Recording instrument compartment

An additional thermocouple was placed in a thermos bottle (fig. 12) containing hot ethylene glycol, the temperature of which was checked with a mercury thermometer just before take-off and just after landing.

Engine cooling, carburetor and oil-cooler air flow, as well as several additional pressure measurements, were made by means of an NACA multiple recording manometer in conjunction with twelve 9-position rotating pressure switches, which made possible the recording of 108 different pressures within about 30 seconds. The installation of the manometer and switches is shown in figures 13 and 14.

For the measurement of engine cooling-air flow, three pressure rakes were set 120° apart in the annular entrance to the engine compartment. Each rake consisted of five impact tubes spaced radially across the opening and one static tube about 1 inch to the side of the center impact tube. Figure 15 shows the right and left rakes.

The pressure at the entrance to the cylinder baffles was measured by a total of 37 impact tubes distributed

between cylinders 1, 3, 4, 6, 7, 9, 10, 12, and 14. Each of these cylinders carried two impact tubes on the exhaust side of the cylinder, one about three fin spaces below and the other about three fin spaces above the bottom of the head; a third tube was in the fins on top of the cylinder head. In addition, cylinders 1, 6, and 10 had impact tubes similarly located on the intake sides of the heads and barrels and cylinders 3 and 4 carried tubes between the topmost concentric head fins and between the lowest barrel fins on the exhaust sides of the cylinders. Some of the tubes in the baffles of cylinders 9 and 10 are indicated by arrows in figure 16. The pressure rake shown was installed after completion of the tests reported herein and preparatory to tests of a blower-cooled installation. Static pressure behind the engine cylinders was measured by open-end tubes sheltered from direct air flow behind and just below each of the nine cylinders on which the impact tubes were placed.

The air flow and the ram to the carburetor were determined by means of a rake (see fig. 17) of five impact tubes on the vertical center line of the scoop about 2 inches behind the center line of the rear cylinders and three static tubes about 1 inch to the side of the impact tubes. Holes flush with the top and bottom walls of the duct gave the static pressure in the boundary layer. Connections were also made to the carburetor impact-pressure tubes below the screen and to the pressure in the float chamber, beyond the altitude compensator.

Pressures in front of the oil cooler (fig. 18) were measured by means of three impact and three static tubes disposed along the vertical center line of the oil cooler, their openings being about 3/4 inches in front of the face of the oil cooler. Three impact tubes were placed about $\frac{1}{2}$ inch behind the rear face of the oil cooler, also on the vertical center line, and a shielded impact tube accurate to about 20° of yaw was set in the exit air stream at the trailing edge of the oil-cooler flap (fig. 19). The relative locations of points of pressure measurement are indicated in figures 6 and 20.

Additional pressure measurements include accessory-compartment, recording-instrument-compartment, and pilot's-cockpit pressures, as well as free-stream impact pressure.

All impact and static tubes to the manometer were of

$\frac{1}{8}$-inch copper tubing, 0.06-inch inside diameter, with leads not less than 12 nor more than 15 feet long.

L-383

Instrument readings made by the pilot included oil-in, carburetor-mixture, and free-air temperatures from vapor-pressure thermometers already installed in the airplane. For the last two flights, a resistance-bulb thermometer with a ratio-type indicator was installed in place of the vapor-pressure free-air thermometer. All free-air thermometers were calibrated for the heating effect due to speed by flying at constant altitude at several airspeeds. The calibrations are shown in figure 21. It was decided that the free-air temperatures recorded by the thermocouple were the most reliable, and these free-air temperatures, corrected for compressibility, are used in this report.

Attempts were made to measure the fuel flow to the engine by two separate methods. One method was by the use of an NACA recording flowmeter installed in the fuel line between the pump and the carburetor; the other was by measuring the pressure drops across the main and economizer jets in the carburetor, which had been calibrated previously on the flow bench. Analysis of the data subsequent to the tests indicated that neither method gave satisfactory results as installed, and no fuel-flow data are presented in this report. It is thought, however, that further development will result in making one or both of those methods of fuel-flow measurement satisfactory and may permit reclamation of the data obtained in these tests.

TEST PROCEDURE

Because the cowling was equipped with only enough cowl-flap area to cool the engine in a medium climb, all full-power testing was confined to the high-speed level-flight condition. The flight tests, then, fell into three groups: first, preliminary ground tests and flights at increasing altitudes and powers to make sure that cooling at full power and critical altitude would be within the allowable limits and to calibrate the airspeed head and free-air thermometer; second, full-power level flights with the original cuffs at several altitudes at and above the engine critical altitude (flights 3-6, 3-8, and 3-9); and third, full-power level flights at approximately the same altitudes as in the second group, but with the cuff angles reduced by about 2° (flights 3-10 and 3-11).

The typical procedure used for testing high speed and cooling pressures may be seen from an inspection of the time histories of the flights (figs. 22, 23, and 24). The pilot made a gentle climb to approximately the rated critical altitude of the engine (14,500 ft), then leveled out, closed the cowl flaps, and went to full throttle at 2700 rpm in the automatic-rich carburetor setting. After reaching constant speed, the pilot switched on the manometer and fuel flowmeter for about 40 seconds, or for slightly more than one cycle of the rotating pressure switches. (All other recording instruments were left on from take-off to landing.) The interval thus covered was considered to be the "run" for purposes of determining the high-speed and cooling characteristics of the airplane at that altitude and power. Upon completion of the run, the pilot would climb to the next altitude (usually about 800 ft higher) and make another run of the same type. In each of the flights for high speed, runs were made at four altitudes. For the last flight with the modified cuffs, one high-speed run was made at an indicated altitude of 17,000 feet in automatic rich, after which the carburetor-mixture control was changed to full rich and then leaned out progressively in order to find whether a higher power could be attained with a different mixture. When the mixture was changed from automatic rich to full rich, the torque dropped 13 percent at constant engine speed; when the mixture was leaned, the torque rose but started to fall off again after almost reaching the value obtained in the automatic rich setting. As it was not considered safe to lean the mixtures below the point at which the torque started to fall off, the pilot immediately set the mixture control back to automatic rich and ended the experiment. A subsequent study of the relative fuel-flow data indicated, however, that the rate of fuel flow to the engine during manual mixture control was never as low as the rate of fuel flow in automatic rich; the unexplored region was indicated to be of the order of 70 pounds of gasoline per hour. The fuel-flow records also indicated that the mixture was becoming slightly richer, rather than leaner, during the last part of the period of manual control.

RESULTS

In figures 22, 23, and 24 are presented time histories of the main high-speed flights, giving the recorded pressure altitude; indicated airspeed; manifold pressure;

torque; engine speed; and head, barrel, and other selected temperatures during the flight. The brake horsepower as calculated from the torque and engine-speed curves is also given.

The periods of steady level flight at different altitudes during which the high speed was being measured are indicated on the time histories. The data pertinent to the determination of maximum speed that were recorded during these runs are plotted to an enlarged scale in figure 25. The values of maximum speed and power calculated from these data for each run are given in table I along with simultaneously recorded data on engine temperatures and cooling and induction air pressures.

DISCUSSION

Maximum Speed

The values of maximum speed given for each run in table I were computed from values of impact and static pressure selected, after inspection of the enlarged time histories of figure 25, as being most representative of steady level flight. Comparison of the values for all runs over the altitude range covered shows a maximum spread of approximately 5 miles per hour in speed. The faired curve of speed against altitude in figure 26 suggests that about 20 percent of this spread is attributable to a consistent variation of speed with altitude. The remaining spread of approximately 4 miles per hour indicates the consistency with which the maximum speed values could be reproduced in different runs under different atmospheric conditions.

The relation between the observed variations of power and speed with altitude shown in figure 26 is most easily understood by consideration of the equilibrium of power required and power available in steady level flight. Under these conditions

$$\frac{DV}{375} = \eta \text{ bhp} \tag{1}$$

or

$$V = 52.73 \left(\frac{\eta}{SC_D}\right)^{1/3} \left(\frac{\text{bhp}}{\sigma}\right)^{1/3} \tag{2}$$

where

D over-all drag of airplane, pounds

V true airspeed, miles per hour

η propulsive efficiency of propeller and exhaust stack combination

bhp brake horsepower

S wing area, square feet

C_D drag coefficient of airplane

σ density ratio

It is immediately apparent that, for full-throttle level flight at and slightly above the critical altitude of an airplane of normal aspect ratio and wing loading and a propeller chosen for good high-speed performance, the value of the parameter $52.73\left(\frac{\eta}{SC_D}\right)^{1/3}$ should be virtually unaffected by moderate changes in weight or altitude. Values of this parameter deduced from the observed values of V and $\frac{bhp}{\sigma}$ for each run are plotted against density altitude in figure 27. As expected, little variation with altitude is apparent.

Under the conditions just described, the parameter $\left(\frac{bhp}{\sigma}\right)^{1/3}$ would also be expected to remain essentially constant over the altitude range covered by the tests. The measured values of this parameter, which are also plotted against density altitude in figure 27, confirm this expectation.

One important phase of the present investigation involves comparison of the high-speed performance of the short-nose cowling and exhaust stack arrangement with that of a similar long-nose version tested previously on the same airplane (reference 4). It has also been suggested that the results might be compared with accepted high-speed performance results for similar airplanes with conventional air-cooled (P-36A) and liquid-cooled (P-40C) in-

L-383

stallations. In order to provide such a comparison, equation (2) in the modified form

$$\left(\frac{V}{52.73}\right)^3 = \left(\frac{\eta}{SC_D}\right)\left(\frac{bhp}{\sigma}\right) \qquad (3)$$

is presented graphically in figure 28. Points representing the high-speed performance of the various airplanes, all of which have the same wing area, are spotted in this figure. The location of a point on the figure immediately reveals not only the maximum speed of the airplane but also the manner by which that speed is attained; that is, by power, supercharging, and ram as indicated by the ordinate scale, or by aerodynamic refinement, as indicated by the abscissa scale.

Within reasonable limits, the figure may be used for several purposes. Primarily, it provides a ready method for determining the effect on maximum speed of changing the critical altitude of an engine installation by either supercharging or ram, or by reducing preheating of the carburetor air. When the corresponding changes in the weight and the propulsive efficiency are small, the effect on the factor $\frac{\eta}{SC_D}$ will be negligible. The abscissa of a point on the figure may therefore be assumed to remain constant while the ordinate is shifted. For instance, for purposes of comparing the cleanness of the two installations in terms of speed at the same horsepower and altitude, it might be assumed that the induction system of the long-nose XP-42 could be modified without increase in drag to get the same high ram as obtained with the short-nose XP-42. In that case, as the same engine was used in both installations, the observed points for the long nose would be shifted upward to the same average value of $\frac{bhp}{\sigma}$ as was observed for the short nose; and the long-nose installation would be expected to attain a maximum speed of 341 miles per hour, compared with the observed maximum speeds of 336 miles per hour for the short nose and 338 miles per hour for the long nose. The chart shows then that the cleanness of the long-nose installation is not fully exploited because of losses in the induction system.

The comparison may be extended to include the P-36A and P-40C, with limitations to be noted later. Inasmuch as the engines of all these airplanes have been rated at

1050 horsepower at various altitudes, it may be assumed that the radial engines could be supercharged to 1050 horsepower at 15,000 feet, or, in other words, to the same power and altitude as that of the P-40C. The comparison would then show:

Airplane	Observed maximum speed (mph)	Maximum speed at 1050 hp at 15,000 ft (mph)
P-40C	347	347
XP-42 long nose	338	352
XP-42 short nose	336	347
P-36A	313	335

This comparison is subject to certain limitations. The engine powers of the P-36A and P-40C were not measured by an engine torque meter and are therefore open to some question. Some additional cooling power would be required to cool the P-36A and the XP-42 engines to the same power rating as the P-40C engine. Comparison of the aerodynamic effect of the engine installation is further complicated by the fact that other sources of drag are not strictly comparable because the gun installations on the XP-42 had been removed and because, on the other hand, some detailed aerodynamic refinements, such as the landing-gear fairing, have been made on the P-40C.

The comparison, however, does appear to indicate that, by use of individual jet exhaust stacks and a high-inlet-velocity cowling, the installation of an air-cooled engine may be made to compare favorably with a conventional liquid-cooled engine installation.

Pressures and Temperatures

The variation of cylinder temperatures around an engine is influenced by a number of factors, such as non-uniform charge and mixture distribution, that are in no way a function of the cowling design. Unless the effect of these factors can be determined, the merit of a cowling designed for general application cannot be reliably

L-383

evaluated by measurements of engine temperatures alone on a specific application. For this reason, primary emphasis in the present tests has been centered on determining the extent to which the type of cowling under consideration provides a high, uniformly distributed pressure over the front of the engine and a suitable, uniformly distributed pressure over the rear of the engine.

Figures 29 to 31 present the results of the pressure and temperature measurements in a graphical form that shows the distribution of both pressure and temperature around the engine for several typical runs. These data indicate that, while pressures at the baffle entrances vary somewhat with the location of the cylinders on which they are measured, they vary even more critically with the point of measurement on the individual cylinder. Values, averaged around the engine, of the front pressures recorded at particular locations in the cylinder baffles are given in table II. They indicate a deficiency of front pressure at the top of the heads of the front cylinders and at the bottom of the barrels of both front and rear cylinders.

In the type of cowling under consideration, in which cooling air is introduced to the engine compartment through a fairly narrow annular opening, the front pressures on the engine, and particularly on the front cylinders, may be expected to vary up and down the cylinder with respect to the location of the entering jet, the magnitude of the variation depending upon the velocity of the jet and the distance of the cylinder behind the jet. If space permits the use of a well-designed diffuser section in the annulus, the jet entering the engine compartment will have negligible velocity head and turbulent losses will also be negligible. The result should then be a high uniform pressure on the front of the engine, the pressure being equal to that in the annulus. If such a diffuser is not or cannot be used, it may reasonably be expected that the maximum variation of front pressures will not exceed the difference between the impact pressure and static pressure of the air at the exit from the diffuser, or, the velocity head of the jet. It is interesting to note in this connection that the lowest pressures measured in the baffles were approximately equal to the measured static pressure in the annulus and that none of the front pressures were as high as the impact pressure in the annulus. The average pressure on the front of the engine was approximately $0.12q_c$ lower than the average impact pressure in the annulus (q_c, airplane impact press.).

The general trend of pressure distribution around the engine indicates that the highest front pressures occurred on the bottom of the engine; whereas the lowest front pressures occurred on the right and the left upper sides of the engine. When average pressures over all high-speed runs are plotted for each common point of pressure measurement, as in figure 32, it is seen that the only points following this trend are the pressures on top of the heads. With the exception of cylinder 3, the distribution of pressure on the side of the heads and barrels was uniform around the engine. The pressure tubes on the side of cylinder 3 were directly behind a large ignition-cable conduit and probably lay in its wake. Although there were usually other obstructions, such as push rods and ignition cables, in front of the other pressure tubes, none were so large as the conduit. These obstructions, however, may account for some of the observed difference in total pressure between the annulus and the engine.

Individual cylinder temperatures showed little tendency to correlate with the pressure drops across the individual cylinders. It may be noted in particular that, although pressures over the top of the front cylinder heads were lower than those over the top of the rear heads, the front head temperatures were lower than those of the rear heads. In this case, the observed pressures on top of the front heads may provide erroneous indications of the air flow, because the tops of the fins, where the pressure tubes were located, were above the direct air jet but the lower halves of the fins were exposed to the jet from the annulus. (See fig. 6.)

An inspection of the cylinder temperatures around the engine shows that the right side of the engine was cooler than the left. The left cylinder heads were on the average, about 35° F hotter than the right, and the left cylinder bases were correspondingly about 10° F hotter than the right. The front base temperatures were slightly higher than the rear base temperatures. There is no apparent explanation why the left side of the engine was hotter than the right, because front and rear cooling-air pressures were nearly uniform.

In figure 33 average head and barrel temperatures in °F above free-air temperature are plotted, along with the cooling-air pressure drops, averaged over the engine, for full-throttle operation over a range of density altitudes above the critical. Also shown are the brake horsepower

and manifold pressure. The change from the original cuffs (flights 3-8 and 3-9) to the modified cuffs (flight 3-10) produced little apparent change in any of the quantities shown. Although individual pressures and temperatures showed little correlation, the variation of average pressures and temperatures was consistent.

A considerable rise in cylinder temperatures at altitudes above critical altitude appears to have resulted from the net effect of decreasing power and decreasing pressure drop. An important probable factor in this temperature rise, however, was the decrease in fuel-air ratio as the manifold pressure decreased at altitudes above the critical altitude. The power compensation of this carburetor depends upon the manifold pressure.

The recommended limiting temperatures for the engine used in these tests were 500° F for the cylinder heads and 335° F for the barrels at the points of measurement used. Army specifications require that the installation be capable of operating within these limiting temperatures under "summer conditions," that is, sea-level temperature is 100° F and the variation of temperature with pressure altitude is 3.6° F per 1000 feet. For correcting tests to these air conditions, a 1:1 temperature correction factor is specified for both heads and barrels. Figure 34 shows the observed head and barrel temperatures in relation to these Army limits. It is immediately apparent that, although head temperatures were relatively low, the maximum barrel temperatures exceeded the Army limits at and above critical altitude even though the engine was operating below its rated military power. A redistribution of available cooling air to provide more pressure at the base of the cylinders would probably correct this condition.*

Figure 35 presents a comparison of the average pressures available at several locations in the cowling. The highest pressures were observed in the carburetor duct,

---

*Subsequent tests on the same engine and thermocouple installation in another short-nose cowling showed that a reduction of 15° F in the temperature of the base thermocouples could be obtained by removal of the baffle sealing strips between the barrels at the bottom of the cylinders. The sealing strips are a special feature of the particular baffle arrangement provided by Pratt & Whitney Aircraft for the engine used in this investigation and are not present in the standard baffle installation for 1830 engines.

where the average pressure was about 104 percent of free-stream impact pressure. This result indicated that the cuffs were loaded even in the high-speed condition. The difference in average pressure between the carburetor duct and the annulus is largely chargeable to the boundary-layer effect on the spinner; whereas the difference between the annulus and the front of the engine, as has been noted, was probably caused by turbulent losses in the rapid expansion from the annulus to the engine compartment. The large boundary-layer effect on the inner edge of the annulus, which forms a continuation of the spinner, may be observed in figure 36, which shows the average pressure distribution in the annulus and in the carburetor duct. The data in table I on impact and static pressures at the surveys in the annular entrance to the engine compartment indicate that the ratio of the velocity head at any point in the survey plane to free-stream impact pressure remained essentially constant over the range of power, altitude, and angle-of-attack conditions covered during the full-throttle high-speed runs. From the faired curves of the ratio of impact and static pressures to free-stream impact pressure, averaged for all three surveys and all high-speed runs as shown in figure 36, it has been found that

$$\int_{\text{inner wall}}^{\text{outer wall}} \sqrt{\frac{\frac{1}{2}\rho_s V_s^2}{q_c}}\, dA = 0.640$$

where

$\frac{1}{2}\rho_s V_s^2$ dynamic pressure at surveys, pounds per square foot

q_c airplane impact pressure, pounds per square foot

A area of annular entrance at survey, square feet

ρ_s air density at survey plane, slugs per cubic foot

V_s air velocity at survey plane, feet per second

The mass flow of air to the engine is

$$\rho_s V_s A = 0.640 \sqrt{2\rho_s q_c}$$

L-383

The volume flow of free air at density ρ_{fa} is

$$\frac{\rho_s V_s A}{\rho_{fa}} = 0.640 \sqrt{\frac{2\rho_s q_c}{\rho_{fa}^2}}$$

Temperature and pressure measurements at the surveys indicate that the density at the surveys ranged from 4 to 6 percent above free-air density so that

$$\text{Volume flow} = 0.928 \sqrt{\frac{q_c}{\rho_{fa}}}$$

Inspection of figure 35 shows that, within the limits of experimental error, the value of $\sqrt{\frac{q_c}{\rho_{fa}}}$ may be taken as 357 at all altitudes covered by the tests. Hence, the flow of cooling air to the engine was 331 cubic feet of free air per second, or 19,860 cubic feet of free air per minute.

Evaluated in a similar manner, the data for the flow in the carburetor duct indicates that

$$\text{Volume flow} = 0.138 \sqrt{\frac{q_c}{\rho_{fa}}} \text{ cubic feet per second}$$

$$= 2960 \text{ cubic feet of free air per minute}$$

Inasmuch as the ratio of horsepower to density was constant, this result leads to the conclusion that the specific air consumption was also nearly constant at 8.9 pounds per brake horsepower-hour.

CONCLUSIONS

Results have been given of high-speed level-flight tests of a short-nose high-inlet-velocity cowling with propeller cuffs on the XP-42 airplane. These results are intended for use in comparisons with other cowlings tested on the same airplane, and for this reason the data obtained have been fully presented.

1. The observed airplane maximum speed was 336 miles per hour at 960 horsepower at 15,000 feet density altitude.

2. Cooling-air pressure recovery on the front of the engine averaged about 80 percent of free-stream impact pressure. The pressure distribution was fairly uniform.

3. With 15 inches of water pressure drop across the engine, the cylinder head temperatures were relatively low, but cylinder base temperatures were slightly above their Army limit.

Langley Memorial Aeronautical Laboratory,
National Advisory Committee for Aeronautics,
Langley Field, Va.

REFERENCES

1. Valentine, E. Floyd: Preliminary Investigation Directed toward Improvement of the NACA Cowling. NACA A.R.R., April 1942.

2. Silverstein, Abe, and Guryansky, Eugene R.: Development of Cowling for Long-Nose Air-Cooled Engine in the NACA Full-Scale Wind Tunnel. NACA A.R.R., Oct. 1941.

3. Pinkel, Benjamin, Turner, L. Richard, and Voss, Fred: Design of Nozzles for the Individual Cylinder Exhaust Jet-Propulsion System. NACA A.C.R., April 1941.

4. Bailey, F. J., Jr., Johnston, J. Ford, and Voglewede, T. J.: Flight Investigation of the Performance and Cooling Characteristics of a Long-Nose High-Inlet-Velocity Cowling on the XP-42 Airplane. NACA A.R.R., April 1942.

L-383

TABLE Ia.-PRESSURE AND TEMPERATURE DATA

	Flight	3-6			3-8				3-9				3-10				3-11
	Run	2	3	4	1	2	3	4	1	2	3	4	1	2	3	4	1
	True airspeed, mph	337	334	333	338	334	336	336	335	335	333	333	336	335	336	335	337
	Density altitude, ft	16950	17000	17800	14900	15800	16550	17300	14950	16000	17050	18300	15250	16000	17100	18050	18000
	Atm press., in. Hg	16.71	16.26	15.74	17.30	16.71	16.16	15.65	17.37	16.58	15.94	15.25	17.26	16.56	15.92	15.26	15.28
	Ambient air temp, °F	21	19	16	15	13	9	5	18	12	10	8	19	13	10	5	5
	Ground air temp, °F	69	69	69	62	62	62	62	78	78	78	78	62	62	62	62	63
	σ, density ratio	.602	.588	.573	.631	.612	.598	.584	.630	.609	.588	.565	.624	.607	.587	.569	.570
	rpm	2680	2680	2680	2680	2680	2680	2680	2680	2680	2680	2680	2700	2700	2700	2700	2700
	bhp	924	905	882	960	933	912	886	956	933	900	872	947	920	884	855	867
	Manifold press., in. Hg	—	—	—	41.2	39.7	38.6	37.6	41.1	39.5	36.0	36.4	41.1	39.7	38.1	36.8	36.8
	q_c, Impact press. in. H_2O	35.4	34.0	33.0	37.3	35.6	34.9	34.2	36.6	35.4	33.7	32.5	36.5	35.4	34.4	33.1	33.5
					Pressure ratio $\frac{p}{q_c}$												
Engine pressure tube locations	1-R	.39	.40	.42	.41	.42	.41	.40	.40	.38	.39	.39	.39	.39	.39	.39	.39
	3-R	.39	.40	.42	.41	.42	.41	.40	.40	.38	.39	.39	.39	.39	.39	.39	"
	4-R	.37	.38	.40	.39	.40	.40	.39	.38	.36	.38	.38	.38	.38	.37	.37	"
	6-R	.39	.39	.41	.41	.42	.41	.40	.40	.38	.39	.39	.39	.40	.39	.39	"
	7-R	"	.40	.42	"	"	"	"	"	"	"	"	"	.39	"	.39	"
	9-R	"	"	"	"	"	"	"	"	"	"	"	"	.40	"	.40	.40
	10-R	"	"	"	"	"	"	"	"	"	"	"	"	"	"	.39	.40
	12-R	"	"	"	"	"	"	"	"	"	"	"	"	"	"	"	.39
	14-R	"	"	"	"	"	"	"	"	"	"	"	"	.39	"	"	.39
	1-TH	.76	.77	.80	.78	.78	.77	.77	.78	.75	.77	.76	.79	.77	.80	.77	.76
	3-TH	.79	.81	.83	.80	.81	.81	.81	.81	.79	.80	.80	.80	.81	.81	.81	.80
	4-TH	.70	.72	.73	.72	.73	.72	.72	.72	.70	.71	.72	.70	.71	.70	.71	.70
	6-TH	.72	.72	.74	.73	.74	.73	.74	.73	.71	.72	.72	.72	.73	.72	.73	.72
	7-TH	.81	.82	.84	.82	.83	.76	.76	.83	.81	.80	.81	.80	.81	.81	.81	.80
	9-TH	.82	.84	.85	.83	.84	.84	.84	.83	.81	.83	.83	.82	.83	.83	.83	.83
	10-TH	.74	.75	.78	.75	.77	.76	.75	.75	.74	.75	.75	.74	.75	.74	.75	.75
	12-TH	.73	.74	.75	.73	.75	.74	.73	.73	.72	.73	.72	.72	.73	.72	.73	.73
	14-TH	.69	.71	.73	.71	.72	.71	.71	.71	.69	.71	.70	.69	.70	.70	.70	.71
	1-EH	.86	.86	.89	.86	.87	.87	.86	.86	.86	.86	.86	—	—	—	—	—
	3-EH	.78	.78	.81	.79	.79	.78	.78	.79	.77	.77	.78	.77	.77	.77	.77	.77
	4-EH	.88	.89	.90	.89	.90	.89	.89	.90	.82	.89	.88	.88	.89	.88	.85	.88
	6-EH	.81	.83	.85	.84	.83	.83	.83	.83	.80	.82	.83	.81	.81	.81	.81	.82
	7-EH	.84	.86	.89	.86	.87	.87	.87	.86	.86	.85	.85	.85	.85	.84	.85	.86
	9-EH	.86	.87	.89	.85	.86	.85	.85	.84	.84	.84	.84	.84	.85	.84	.84	.84
	10-EH	.86	.88	.90	.87	.88	.87	.87	.87	.86	.86	.87	.86	.87	.87	.86	.87
	12-EH	.86	.87	.89	.88	.88	.87	.87	.86	.85	.85	.85	.84	.84	.83	.84	.84
	14-EH	.83	.84	.85	.84	.85	.84	.83	.84	.82	.83	.83	.82	.83	.82	.82	.83
	1-EB	.84	.85	.87	.85	.85	.84	.84	.84	.83	.83	.83	.84	.84	.83	.83	.85
	3-EB	.68	.70	.72	.70	.71	.70	.70	.70	.69	.69	.70	.69	.70	.69	.69	—
	4-EB	.78	.79	.80	.79	.80	.79	.79	.80	.78	.79	.79	.79	.80	.79	.79	.79
	6-EB	.81	.83	.85	.83	.83	.83	.83	.83	.80	.82	.82	.82	.83	.82	.83	.83
	7-EB	.80	.81	.83	.81	.83	.81	.81	.82	.80	.81	.81	.79	.80	.80	.80	.80
	9-EB	.82	.83	.86	.83	.84	.83	.84	.83	.82	.83	.83	.82	.83	.82	.83	.83
	10-EB	.77	.77	.80	.78	.80	.79	.79	.78	.77	.77	.77	.80	.78	.77	.78	.79
	12-EB	.78	.80	.82	.80	.80	.80	.80	.79	.78	.79	.78	.79	.80	.78	.79	.79
	14-EB	.78	.80	.82	.80	.80	.80	.80	.79	.78	.79	.78	.78	.80	.78	.79	.79
	1-IH	.82	.82	.84	.82	.84	.82	.82	.81	.81	.81	.82	.81	.81	.81	.82	.82
	6-IH	.87	.88	.90	.89	.90	.88	.89	.89	.86	.85	.88	.88	.88	.88	.88	.89
	10-IH	.89	.91	.93	.91	.93	.91	.92	.90	.89	.90	.90	.91	.92	.91	.91	.91
	1-IB	.77	.78	.81	.79	.78	.78	.78	.78	.77	.78	.77	.78	.77	.76	.77	.78
	6-IB	.85	.86	.88	.86	.87	.86	.85	.86	.85	.85	.85	.85	.85	.85	.85	.86
	10-IB	.82	.82	.85	.83	.83	.82	.82	.83	.82	.82	.82	.83	.82	.81	.82	.84
	3-EH2	.78	.80	.82	.80	.80	.79	.80	.80	.78	.79	.80	.79	.81	.80	.80	.79
	4-EH2	.86	.86	.89	.88	.89	.88	.87	.89	.86	.86	.87	.85	.86	.84	.85	.86
	3-EB2	.64	.66	.67	.66	.67	.66	.66	.65	.64	.68	.65	.64	.65	.64	.64	.65
	4-EB2	.67	.69	.72	.68	.69	.68	.68	.66	.66	.67	.66	.69	.70	.67	.71	.69

Sheltered tubes behind engine

Top of head

Exhaust side of head

Exhaust side of barrel

Intake side of head

Intake side of barrel

Method of designating tube locations for typical cylinders

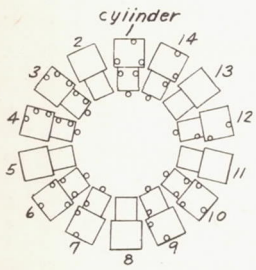

Cylinder 1.

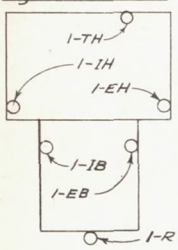

Cylinder 3.

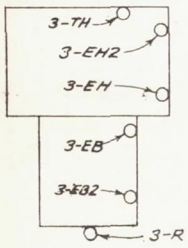

TABLE Ib.-PRESSURE AND TEMPERATURE DATA

	Flight	3-6			3-8				3-9				3-10				3-11
	Run	2	3	4	1	2	3	4	1	2	3	4	1	2	3	4	1
	True air speed, mph	337	334	333	338	334	336	336	335	335	333	333	336	335	336	335	337
	Density altitude, ft	16350	17100	17800	14900	15800	16550	17300	14950	16000	17050	18300	15250	16000	17100	18050	18000
	Atm. press., in Hg	16.71	16.26	15.74	17.30	16.71	16.16	15.65	17.37	16.58	15.94	15.25	17.26	16.56	15.92	15.26	15.28
	Ambient air temp, °F	21	19	16	15	13	9	5	18	12	10	8	19	13	10	5	5
	Ground air temp, °F	69	69	69	62	62	62	62	78	78	78	78	62	62	62	62	63
	σ, density ratio	.602	.588	.573	.631	.612	.598	.584	.630	.609	.588	.565	.624	.607	.587	.569	.570
	rpm	2680	2680	2680	2680	2680	2680	2680	2680	2680	2680	2680	2700	2700	2700	2700	2700
	bhp	924	905	882	960	933	912	886	956	933	900	872	947	920	884	855	867
	Manifold press, in. Hg	—	—	—	41.2	39.7	38.6	37.6	41.1	39.5	38.0	36.4	41.1	39.7	38.1	36.8	36.8
	q_c, impact press in. H_2O	35.4	34.0	33.0	37.3	35.6	34.9	34.2	36.6	35.9	33.7	32.5	36.5	35.9	34.4	33.1	33.5
		Pressure ratio, p/q_c															
Annulus pressure tube locations	A-TP1 (Top survey, Impact tubes)	.84	.86	.88	.85	.86	.85	.85	.85	.84	.84	.84	.85	.86	.85	.85	.86
	A-TP2	.92	.95	.90	.94	.95	.94	.93	.93	.93	.93	.93	—	—	—	—	.93
	A-TP3	.94	.97	.98	.97	.98	.95	.94	.96	.94	.96	.95	.95	.97	.95	.96	.96
	A-TP4	.95	.97	.98	.98	.96	.97	.97	.97	.95	.96	.95	.95	.96	.95	.97	.97
	A-TP5	.90	.94	.98	.91	.92	.90	.90	.93	.92	.92	.92	.90	.91	.90	.90	.90
	A-TS (Static tube)	.66	.66	.68	.68	.68	.67	.67	.67	.66	.66	.67	.66	.67	.66	.67	.67
	A-RP1 (Right survey, Impact tubes)	.84	.86	.88	.84	.86	.85	.84	.85	.83	.83	.84	.83	.83	.83	.84	.82
	A-RP2	.92	.95	.90	.94	.95	.95	.94	.95	.94	.94	.94	.93	.94	.93	.95	.93
	A-RP3	.97	.98	1.00	.99	1.00	.98	.98	.99	.97	.98	.99	.96	.97	.97	.97	.97
	A-RP4	.97	.97	.99	.97	.98	.97	.97	.99	.97	.97	.97	.95	.96	.95	.96	.96
	A-RP5	.89	.90	.92	.90	.90	.89	.88	.90	.89	.89	.88	.88	.89	.88	.88	.88
	A-RS (Static tube)	.66	.66	.68	.68	.68	.67	.67	.67	.66	.69	.67	.66	.67	.66	.67	.67
	A-LP1 (Left survey, Impact tubes)	.86	.88	.89	.87	.87	.86	.86	.85	.86	.86	.84	.86	.86	.85	.86	.87
	A-LP2	.94	.96	.91	.96	.95	.95	.94	.96	.94	.95	.95	.96	.95	.94	.96	.95
	A-LP3	.98	.99	1.01	1.00	1.00	.99	.99	.99	.97	.99	.99	.96	.97	.97	.97	.98
	A-LP4	.97	.97	1.00	.98	.99	.98	.98	.96	.97	.97	.97	.98	.99	.98	.98	.98
	A-LP5	.86	.87	.89	.87	.87	.86	.87	.87	.85	.85	.86	.87	.88	.86	.87	.87
	A-LS (static tube)	.72	.73	.75	.73	.74	.73	.73	.74	.72	.73	.73	.71	.72	.71	.72	.73
Oil cooler pressure tube locations	O-FP1 (Front survey, Impact tubes)	1.01	1.01	1.04	.99	.99	.98	.99	.99	.97	.97	.99	.96	.97	.98	.97	1.01
	O-FP2	1.04	1.04	1.06	1.03	1.03	1.03	1.03	1.03	1.02	1.08	1.03	1.02	1.00	.97	1.03	1.04
	O-FP3	1.04	1.05	1.06	1.05	1.05	1.05	1.05	1.05	1.04	1.04	1.05	1.04	1.03	—	—	1.05
	O-FS1 (Static tubes)	.91	.92	.93	.93	.93	.92	.92	.92	.90	.91	.92	.90	.91	.92	.91	.93
	O-FS2	.92	.93	.94	.93	.93	.92	.94	.94	.91	.92	.93	.91	.91	.92	.92	.93
	O-FS3	.94	.94	.96	.94	.94	.94	.95	.94	.94	.93	.94	.92	.93	.93	.94	.96
	O-RP1 (Rear survey, impact tubes)	.71	.71	.73	.71	.72	.71	.71	.72	.69	.71	.71	.70	.71	.69	.70	.72
	O-RP2	.81	.83	.85	.83	.83	.83	.82	.83	.80	.83	.82	.81	.81	.81	.82	.83
	O-RP3	.59	.61	.63	.60	.61	.60	.60	.59	.58	.59	.60	.58	.59	.59	.60	.62
	O-SP (Shielded impact tube)	.59	.60	.62	.60	.60	.60	.59	.59	.57	.58	.59	.58	.59	.58	.59	.60
Carburetor scoop pressure tube locations	C-P1 (Impact tubes)	1.02	1.02	1.04	1.03	1.04	1.02	1.03	1.03	1.02	1.01	1.02	1.01	1.01	1.01	1.01	1.01
	C-P2	1.03	1.04	1.06	1.03	1.04	1.03	1.04	1.05	1.04	1.03	1.03	1.02	1.02	1.02	1.02	1.02
	C-P3	1.04	1.06	1.07	1.05	1.06	1.04	1.05	1.05	1.04	1.04	1.05	1.03	1.05	1.04	1.03	1.04
	C-P4	1.05	1.07	1.09	1.07	1.07	1.06	1.06	1.07	1.05	1.05	1.05	1.04	1.05	1.04	1.04	1.04
	C-P5	1.06	1.07	1.09	1.07	1.07	1.06	1.06	1.07	1.05	1.06	1.06	1.04	1.05	1.05	1.05	1.04
	C-S1 (Static tubes)	.86	.86	.88	.86	.87	.87	.86	.86	.85	.86	.86	.85	.85	.84	.84	.86
	C-S2	.84	.84	.86	.84	.85	.84	.84	.84	.84	.84	.84	.82	.83	.83	.83	.83
	C-S3	.83	.84	.87	.84	.84	.84	.84	.84	.82	.83	.84	—	—	—	—	—
	C-S4	.84	.84	.87	.84	.85	.84	.84	.85	.83	.84	.84	.82	.83	.82	.83	.84
	C-S5	.84	.85	.87	.84	.85	.84	.85	.85	.84	.84	.84	.83	.83	.83	.83	.84

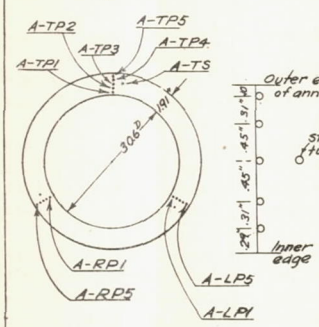

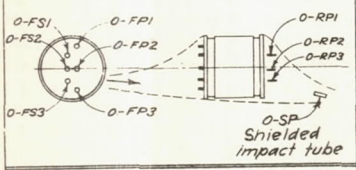

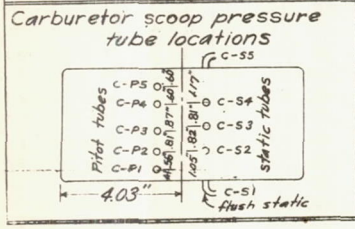

TABLE Ic.-PRESSURE AND TEMPERATURE DATA

Test - Flight Run	3-6			3-8				3-9				3-10				3-11
	2	3	4	1	2	3	4	1	2	3	4	1	2	3	4	1
True airspeed, mph	337	334	333	338	334	336	336	335	335	333	333	336	335	336	335	337
Density altitude, ft	16350	17000	17800	14900	15800	16550	17300	14950	16000	17050	18300	15250	16000	17100	18050	18000
Atm press, in. Hg	16.71	16.26	15.74	17.30	16.71	16.16	15.65	17.37	16.58	15.94	15.25	17.26	16.56	15.92	15.26	15.28
Ambient air temp, °F	21	19	16	15	13	9	5	18	12	10	8	19	13	10	5	5
Ground air temp, °F	69	69	69	62	62	62	62	78	78	78	78	62	62	62	62	63
σ, density ratio	.602	.588	.573	.631	.612	.598	.584	.630	.609	.588	.565	.624	.607	.587	.569	.570
rpm	2680	2680	2680	2680	2680	2680	2680	2680	2680	2680	2680	2700	2700	2700	2700	2700
bhp	924	905	882	960	933	912	886	956	933	900	872	947	920	884	855	867
Manifold press, in. Hg	—	—	—	41.2	39.7	38.6	37.6	41.1	39.5	38.0	36.4	41.1	39.7	38.1	36.8	36.8
q_c, impact press in. H_2O	35.4	34.0	33.0	37.3	35.6	34.9	34.2	36.6	35.4	33.7	32.5	36.5	35.4	34.9	33.1	33.5
Cylinder—point of measurement	**Temperature °F**															
1 — gasket thermocouple at rear spark plug	thermocouple broken															
2	392	392	403	388	388	390	403	370	370	379		382	384	393	398	396
3	405	390	403	399	—	397	410	385	385	388		395	392	395	400	400
4	392	392	399	396	388	390	397	374	374	379		384	384	388	391	391
5	ermocouple			broken												
6	367	369	392	365	365	369	376	360	363	367		366	362	366	369	370
7	430	428	435	421	424	424	430	417	419	419		418	422	425	429	425
8	383	381	390	381	379	387	387	365	372	370		373	375	378	382	386
9	415	419	424	406	408	408	419	397	403	403		405	407	407	407	406
10	421	428	432	414	415	421	428	410	412	415		418	418	422	422	411
11	428	430	437	424	423	428	433	415	415	417		418	422	423	429	422
12	403	405	414	399	399	405	412	394	394	397		400	400	405	405	406
13	424	428	435	419	421	424	433	412	415	417		420	422	429	431	431
14	423	424	432	414	415	419	428	405	405	410		414	414	418	423	422
1 — rear ¼ of flange at base of cylinder	thermocouple broken															
2	311	309	311	302	302	302	311	297	297	300		301	303	307	308	308
3	300	300	302	293	293	295	300	288	286	288		294	296	296	298	299
4	302	302	304	295	293	295	300	286	286	288		295	298	299	298	296
5	288	288	289	282	284	286	288	275	275	279		287	287	287	287	287
6	304	304	306	297	297	300	304	293	289	293		303	303	303	303	303
7	293	293	295	286	286	289	291	279	280	282		289	290	290	290	288
8	295	295	297	293	289	293	295	286	286	288		289	290	290	290	294
9	306	311	311	302	302	302	307	295	297	300		301	303	303	303	305
10	320	325	324	316	316	318	320	309	309	311		314	316	319	319	317
11	293	297	297	286	286	288	293	286	282	288		289	290	294	290	294
12	311	320	324	309	311	313	318	304	304	306		310	312	314	314	314
13	300	302	304	296	295	297	324	293	289	293		296	299	303	303	303
14	311	311	311	304	304	302	313	297	297	300		305	307	308	308	305
10 — intake port	225	225	225	217	217	217	217	214	210	210		217	217	215	215	215
Mixture at blower rim	163	156	163	156	154	151	149	147	147	147	no temperature record	159	157	154	154	146
Fuel on suction side of pump	77	81	84	81	82	86	86	77	73	77		71	71	71	78	78
" " pressure " " "	84	90	90	82	86	86	86	81	77	81		78	82	78	86	78
" at outlet of flow meter	88	93	93	86	86	90	90	84	84	84		82	83	82	87	80
" in carburetor float chamber	84	88	90	86	86	82	86	77	75	75		78	78	82	82	78
1 — front spark plug elbow	46	46	46	68	39	39	39	68	68	68		49	49	49	49	40
1 — rear " " "	88	84	88	81	77	77	72	72	68	68		78	78	74	71	71
7 — front " " "	46	46	46	39	39	39	39	46	48	55		49	49	46	49	40
7 — rear " " "	55	54	54	52	52	48	39	46	43	36		53	49	46	40	40
11 — front " " "	50	46	46	46	46	43	39	43	39	36		49	46	40	37	36
11 — rear " " "	81	81	81	77	77	77	72	68	68	68		78	78	74	71	71
Recorded free air	39	38	34	33	32	27	23	36	30	25		37	31	28	23	23
Pilot's observed free air	37	35	33	36	33	31	29	35	32	29	25	31	29	25	20	19
Air in carburetor scoop	46	46	46	46	39	39	36	39	36	30		46	42	37	33	31
" at top annular rake	46	46	46	46	39	39	36	39	36	32		46	40	37	33	31
" in front of cylinder 1.	54	54	50	52	48	48	43	46	39	36		49	49	46	40	40
" behind cylinder 1.	183	192	190	172	169	176	167	131	—	—		—	—	—	—	
" at exit from oil cooler	81	81	81	77	72	70	72	68	61	57		74	71	69	62	62
Oil in line	138	138	138	133	133	131	133	131	133	129		134	134	132	132	132
" out	214	214	214	208	208	207	207	203	201	201		206	206	208	204	200
Accessory compartment	126	129	129	124	120	118	122	109	106	106		119	119	116	116	110
Right magneto	thermocouple broken															
Left "	108	108	108	106	106	104	102	97	93	97		107	103	103	100	100
Pilot's cockpit (recorded)	90	97	97	90	90	90	86	88	88	84		91	87	89	87	78
" " (observed)	—	—	—	90	90	90	89	86	86	85	84	—	—	—	—	79
Recording instrument compartment	88	93	93	86	86	86	84	81	81	77		87	87	85	85	74

L-383

TABLE II

AVERAGE COOLING AIR PRESSURES AT SEVERAL LOCATIONS ON FRONT AND REAR CYLINDERS

Locations	Flight	3-6			3-8				3-9				3-10				3-11
	Run	2	3	4	1	2	3	4	1	2	3	4	1	2	3	4	
		Average pressure, p/q_c															
Top of heads	Front cylinder	0.72	0.73	0.75	0.73	0.74	0.73	0.73	0.73	0.71	0.72	0.72	0.71	0.72	0.72	0.72	0.72
	Rear cylinder	.80	.81	.83	.81	.82	.80	.80	.81	.79	.80	.80	.80	.81	.81	.81	.80
Exhaust side of heads	Front cylinder	.85	.86	.88	.86	.87	.86	.86	.86	.83	.85	.85	.84	.85	.84	.84	.85
	Rear cylinder	.84	.84	.87	.84	.85	.84	.84	.84	.83	.83	.83	.82	.82	.82	.82	.82
Exhaust side of barrels	Front cylinder	.78	.80	.82	.80	.81	.80	.80	.80	.78	.79	.79	.80	.80	.79	.80	.80
	Rear cylinder	.79	.80	.82	.80	.81	.80	.80	.80	.79	.79	.79	.79	.79	.79	.79	.83
Intake side of heads	Front cylinder[1]	.88	.90	.92	.90	.92	.90	.91	.90	.88	.88	.89	.90	.90	.90	.90	.90
	Rear cylinder[2]	.82	.82	.84	.82	.84	.82	.82	.81	.81	.81	.82	.81	.81	.81	.82	.82
Intake side of barrels	Front cylinder[1]	.84	.84	.87	.85	.85	.84	.84	.85	.84	.84	.84	.84	.84	.83	.84	.85
	Rear cylinder[2]	.77	.78	.81	.79	.78	.78	.78	.78	.77	.78	.77	.78	.77	.76	.77	.78
Topmost fin on exhaust side of heads	Front cylinder[3]	.86	.86	.89	.88	.89	.88	.87	.89	.86	.86	.87	.85	.86	.84	.85	.86
	Rear cylinder[4]	.78	.80	.82	.80	.80	.79	.80	.80	.78	.79	.80	.79	.81	.80	.80	.79
Lowest fin on exhaust side of barrels	Front cylinder[3]	.67	.69	.70	.68	.69	.68	.68	.66	.66	.67	.66	.69	.70	.67	.71	.69
	Rear cylinder[4]	.64	.66	.67	.66	.67	.66	.66	.65	.64	.68	.65	.64	.65	.64	.64	.65

[1]Based on cylinders 6 and 10.
[2]Based on cylinder 1.
[3]Based on cylinder 4.
[4]Based on cylinder 3.

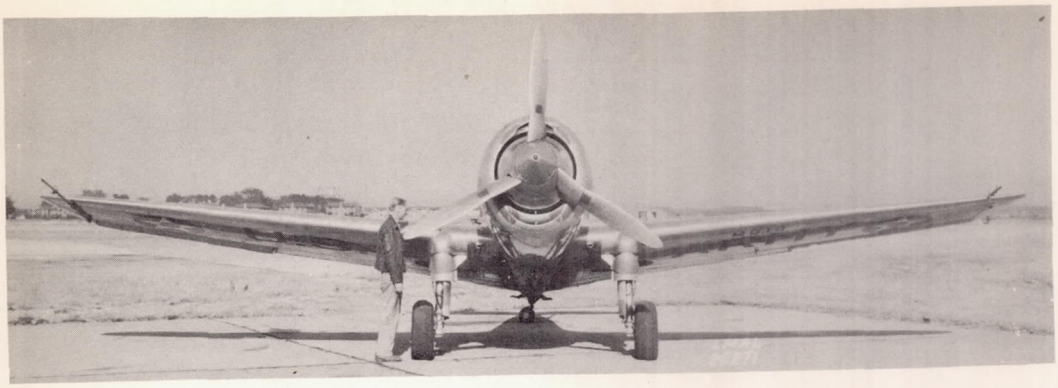

Figure 1.- Front view of XP-42 airplane with short-nose high-inlet-velocity cowling.

Figure 2.- Three-quarter front view of the XP-42 airplane with short-nose high-inlet-velocity cowling.

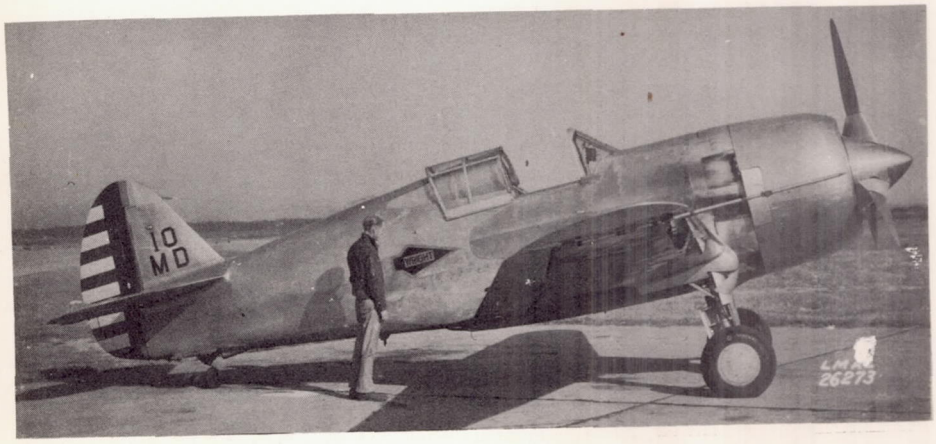

Figure 3.- Side view of the XP-42 airplane with short-nose high-inlet-velocity cowling.

L-383

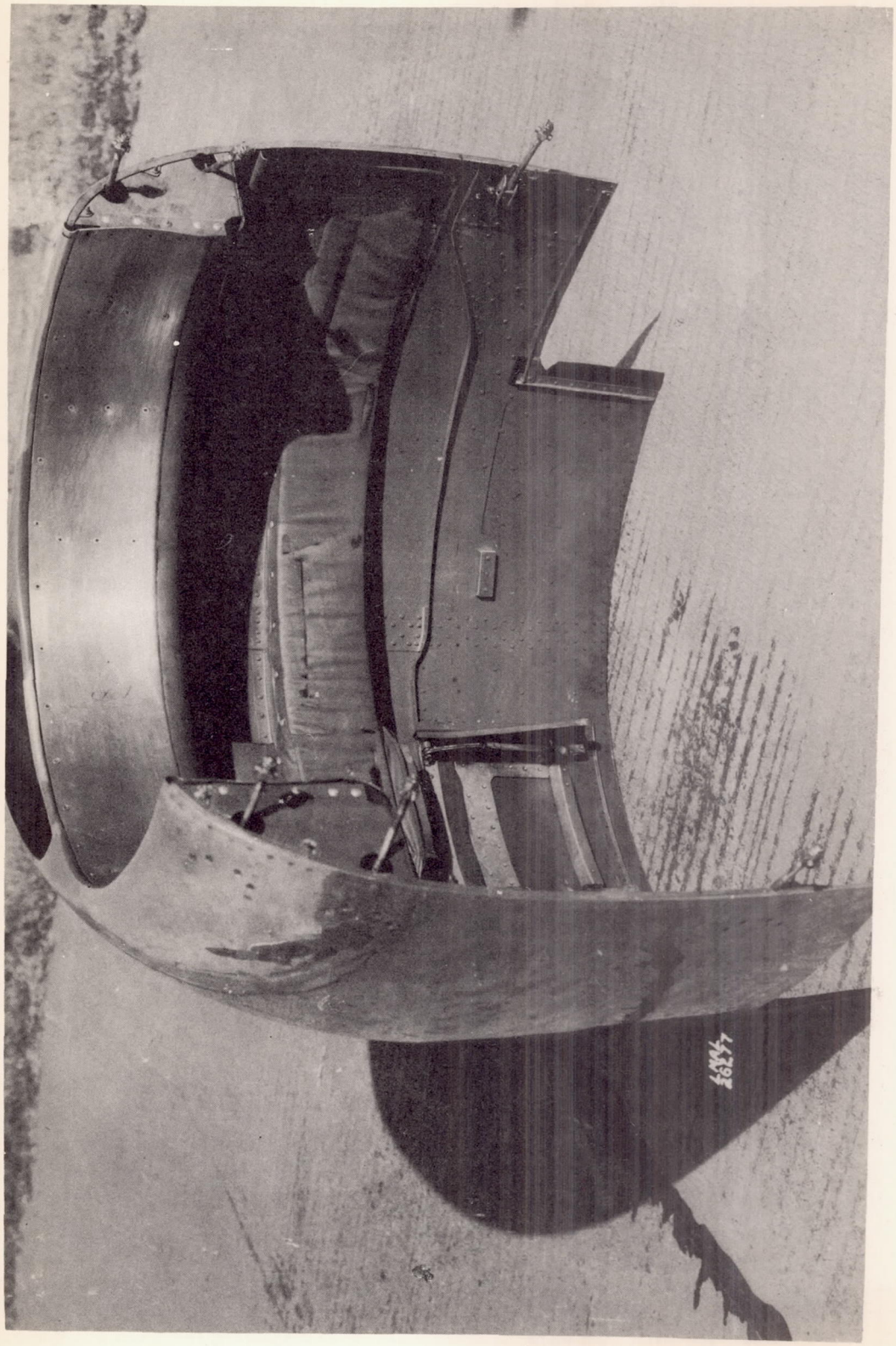

Figure 4.- Upper part of short-nose high-inlet-velocity cowling.

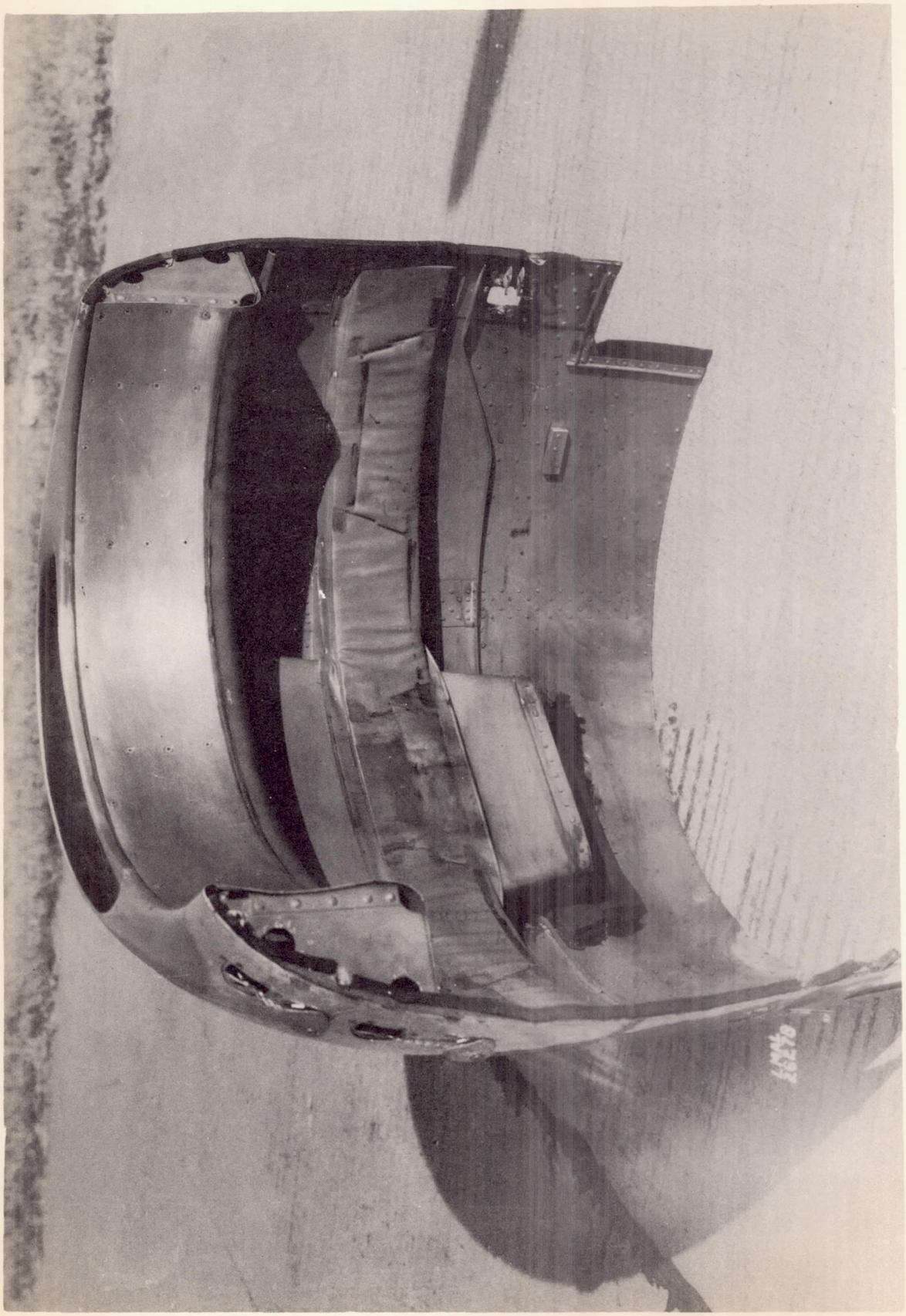

Figure 5.- Lower part of short-nose high-inlet-velocity cowling.

L-383

NACA

FIG. 6 XP-42 SHORT NOSE HIGH INLET SPEED COWLING.

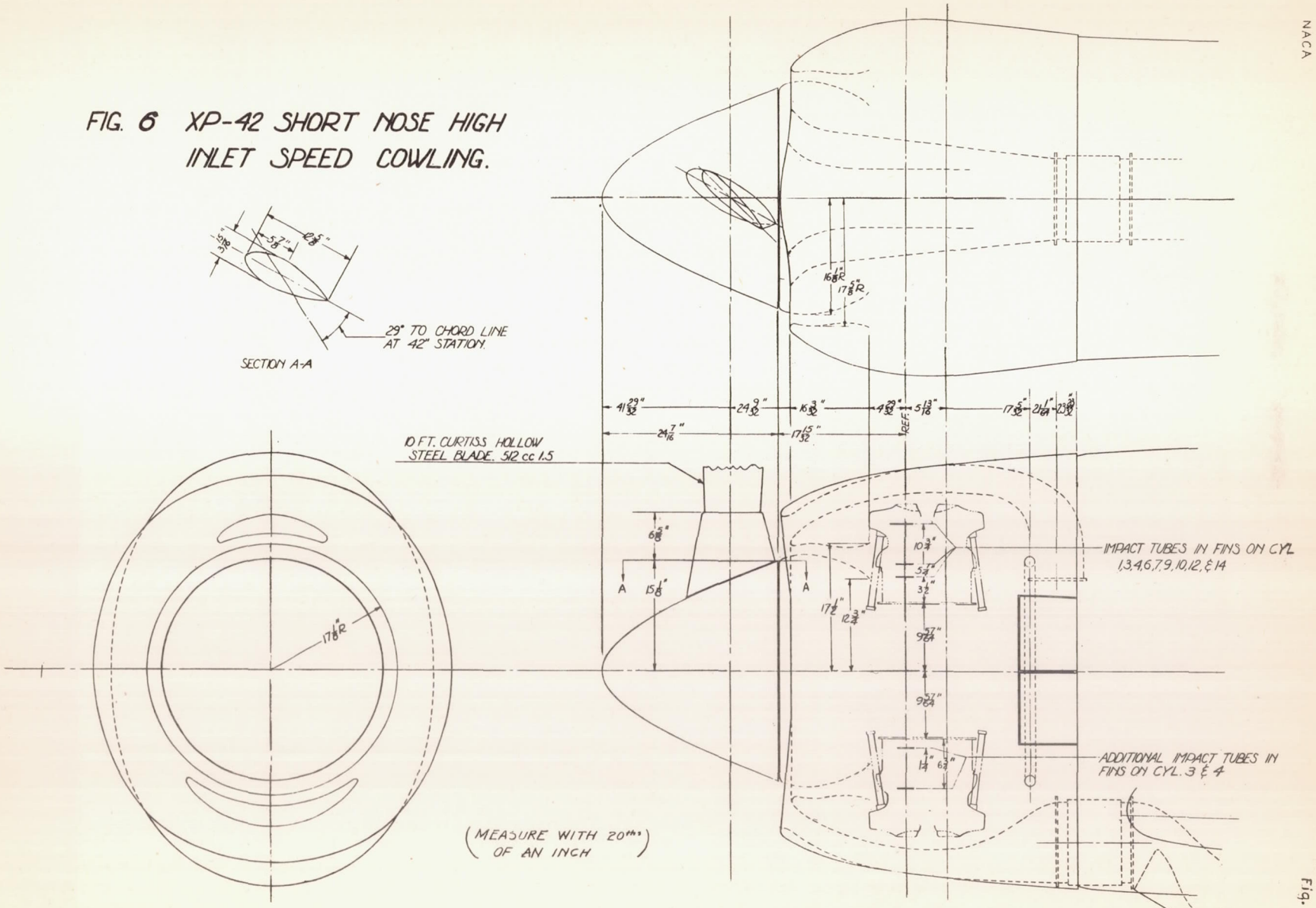

Fig. 6

L-353

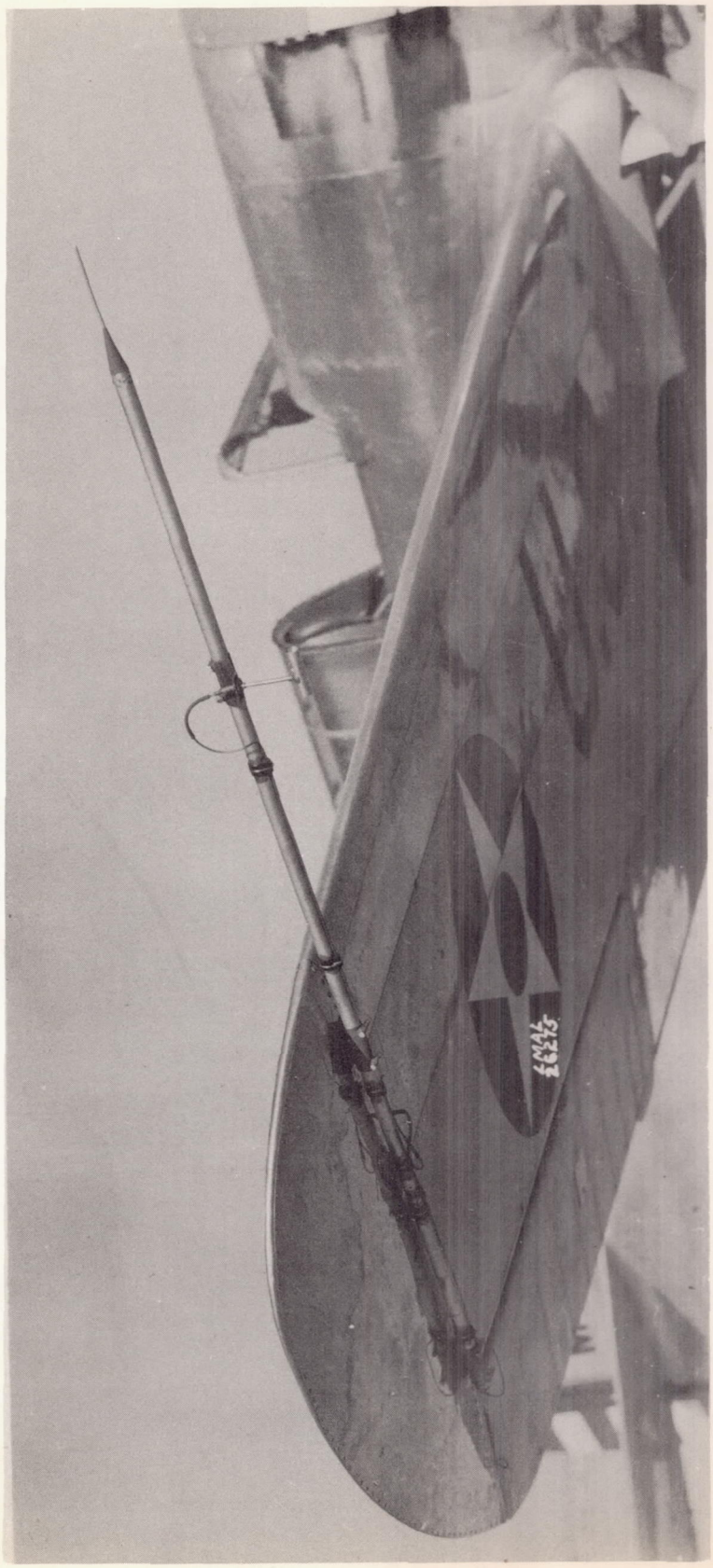

Figure 7.- Airspeed boom on right wing.

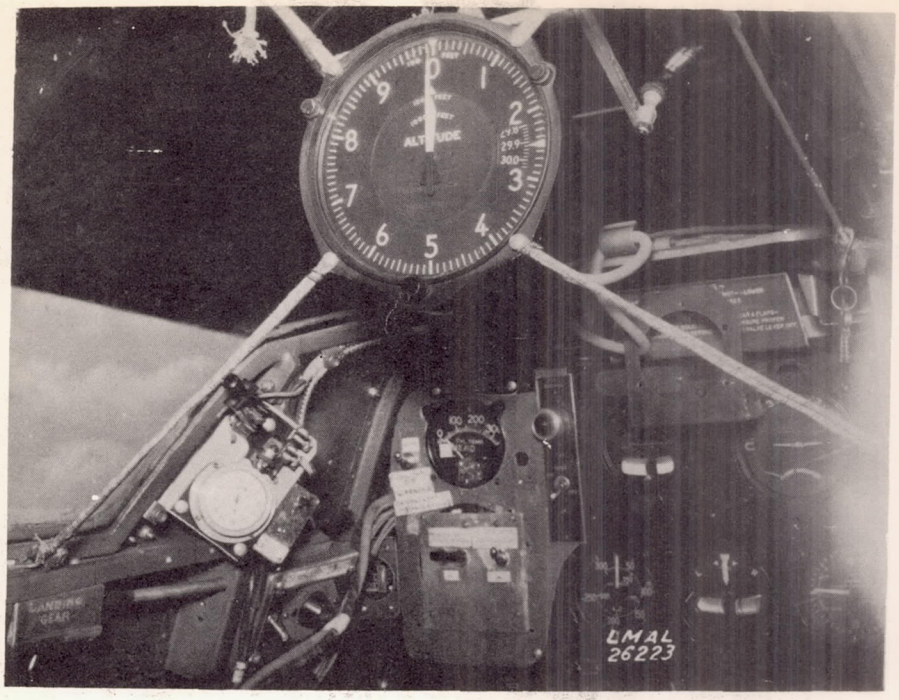

Figure 8.- Sensitive altimeter used in calibrating airspeed head.

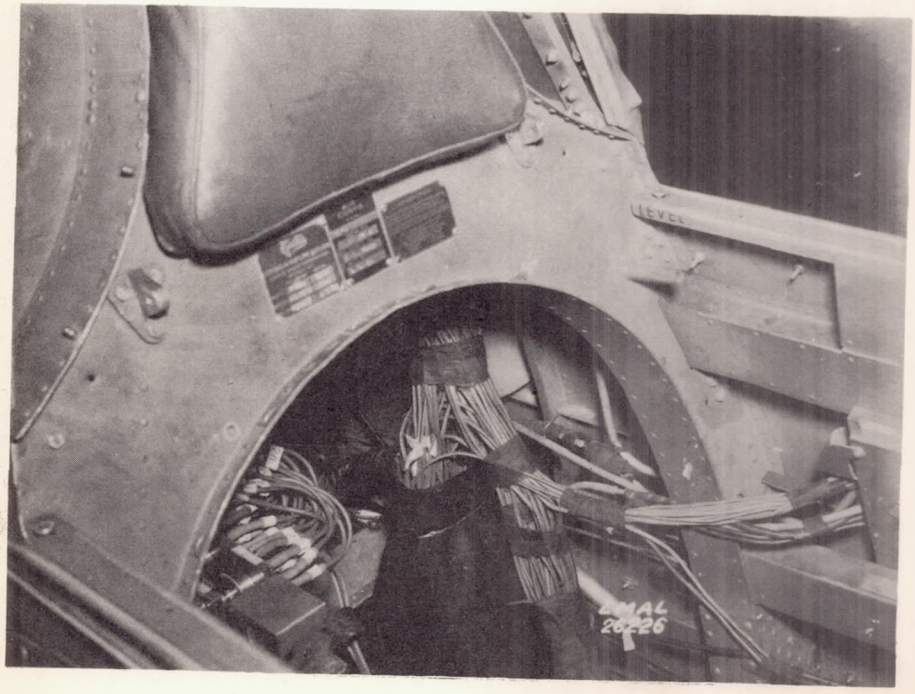

Figure 9.- Thermocouple leads to cold-junction box.

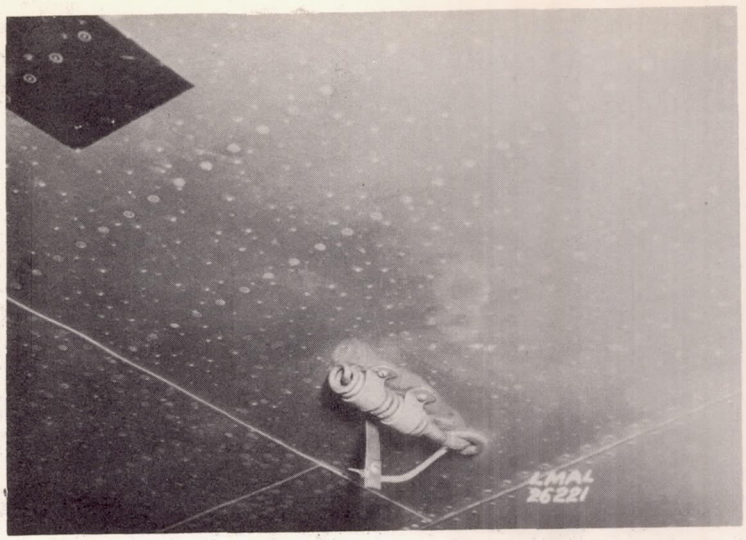

Figure 10.- Free-air thermocouple and vapor-pressure thermometer.

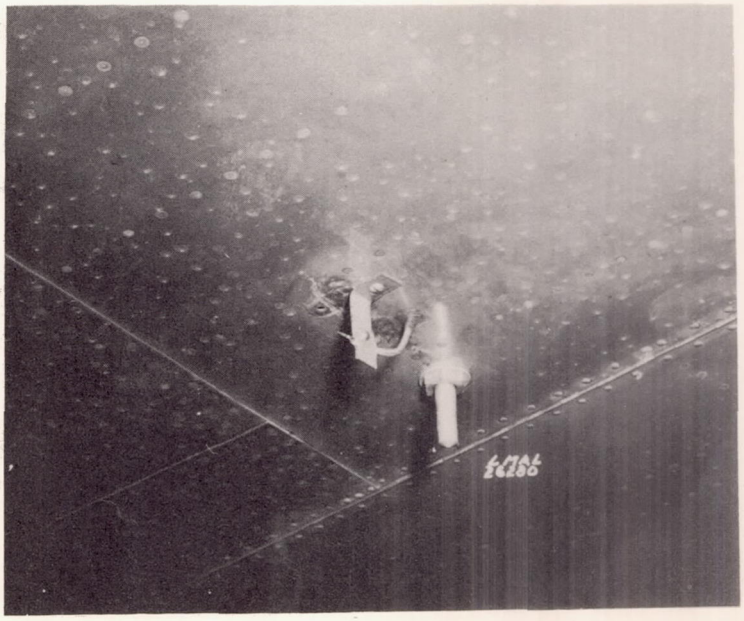

Figure 11.- Free-air thermocouple and resistance-bulb thermometer.

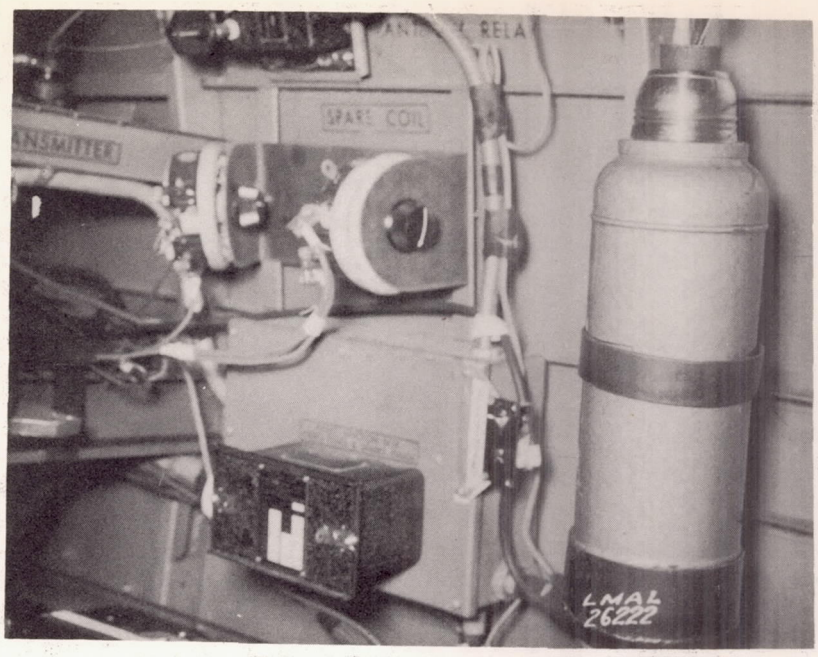

Figure 12.- Thermos bottle used as hot junction.

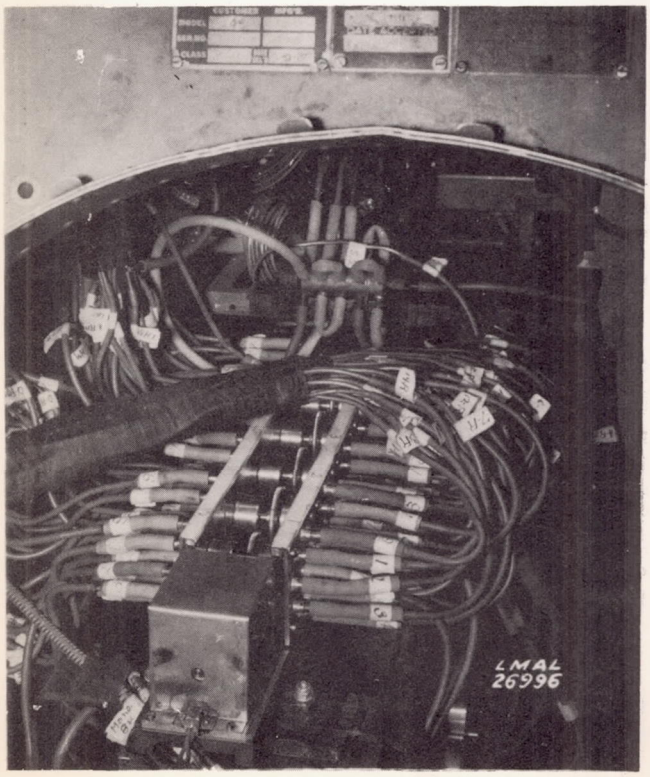

Figure 13.- Pressure-switch installation over manometer.

L-383

L-353

Figure 14.- Manometer and pressure-switch installation.

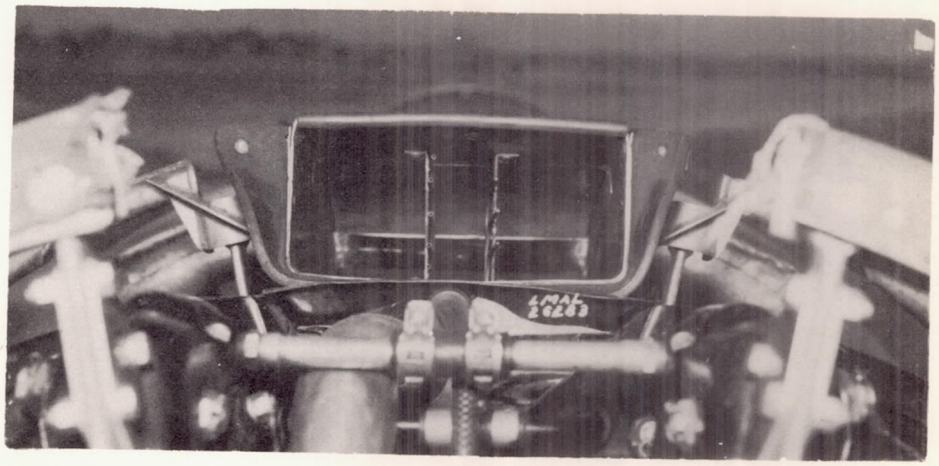

Figure 17.- Rear part of carburetor duct, showing pressure rakes.

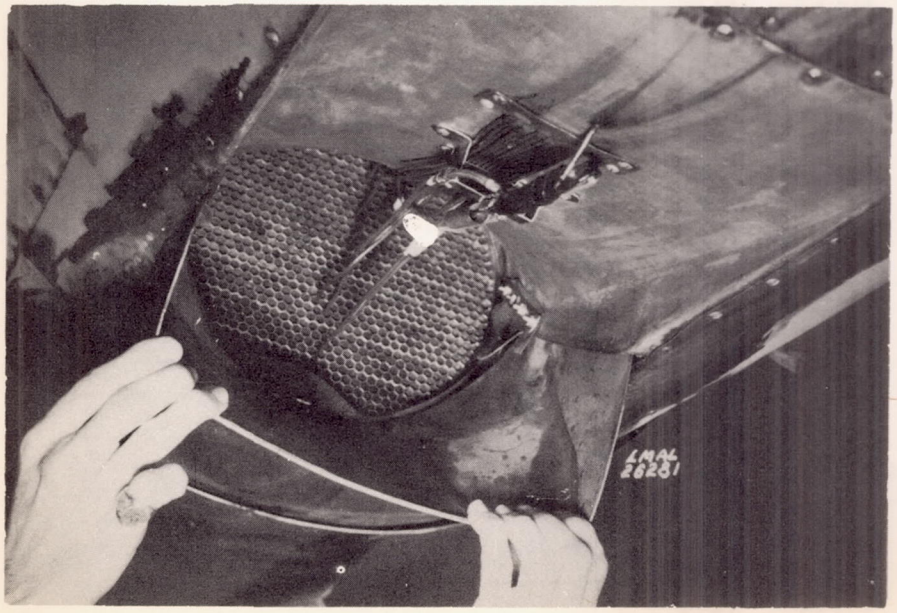

Figure 19.- Rear of oil cooler.

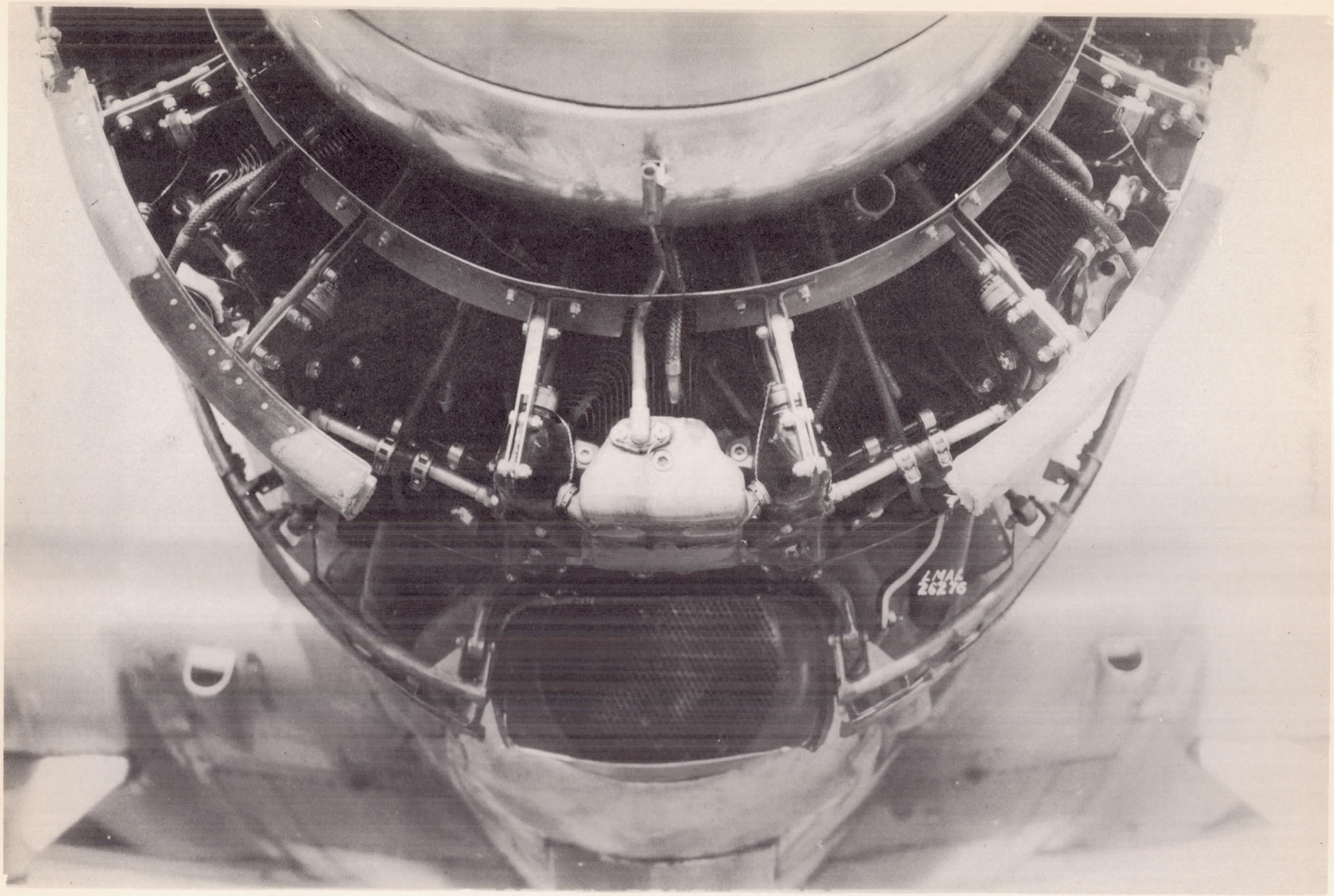

Figure 15.- Front of engine with cowling removed, showing right and left pressure rakes in annulus.

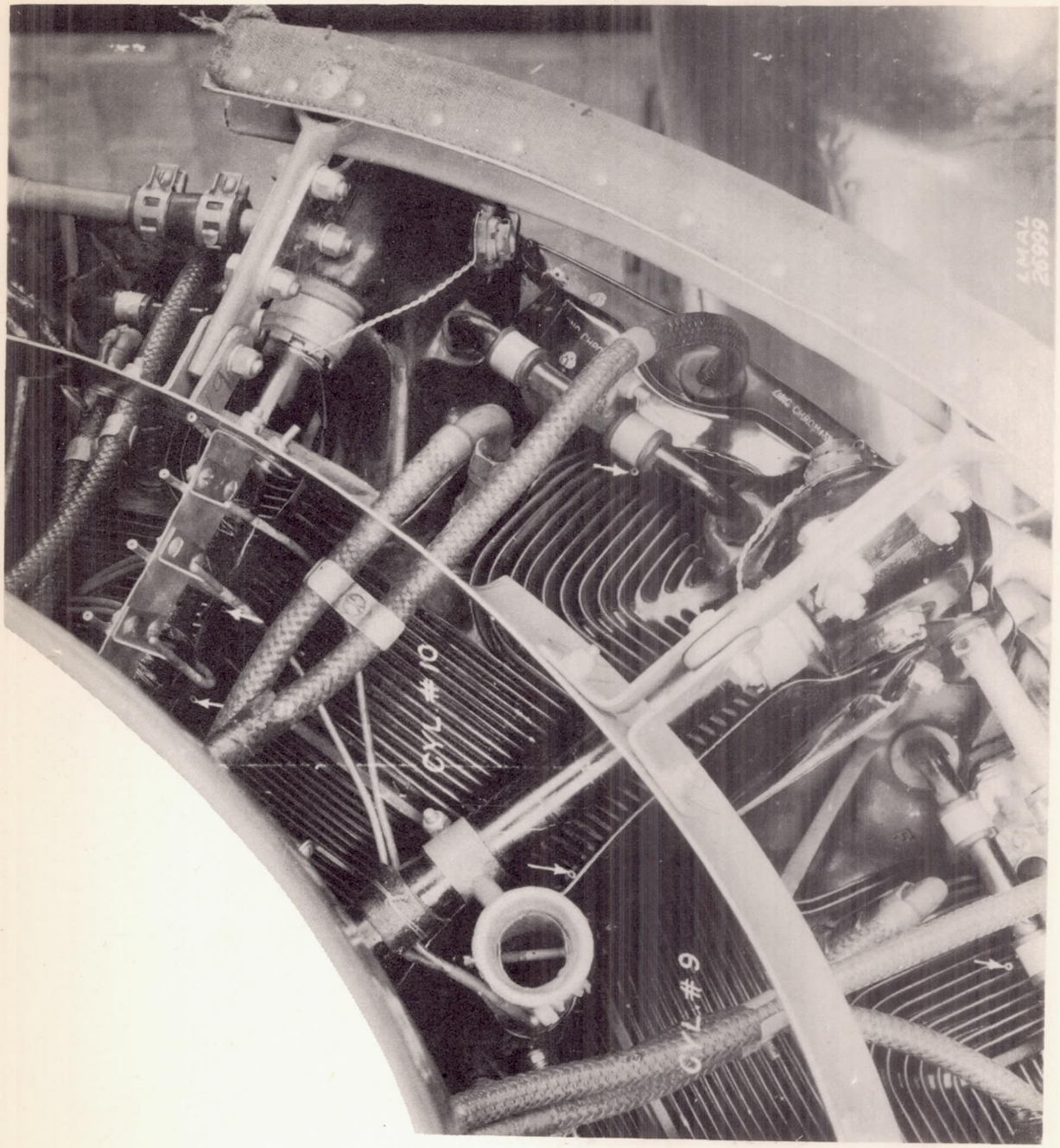

Figure 16.- Pressure tubes in baffles of cylinder 10.

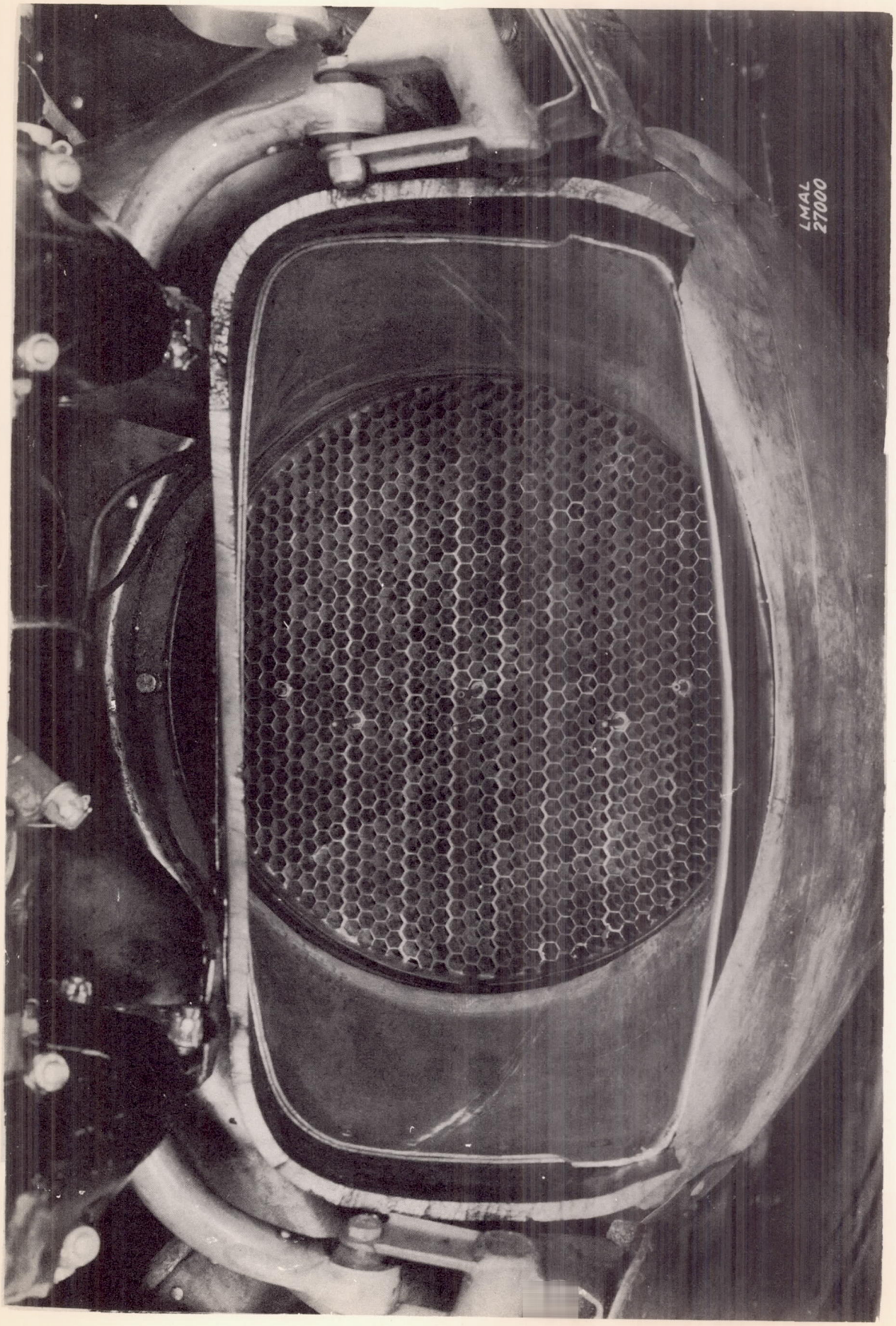

Figure 18.- Face of oil cooler, showing pressure tubes.

L-383

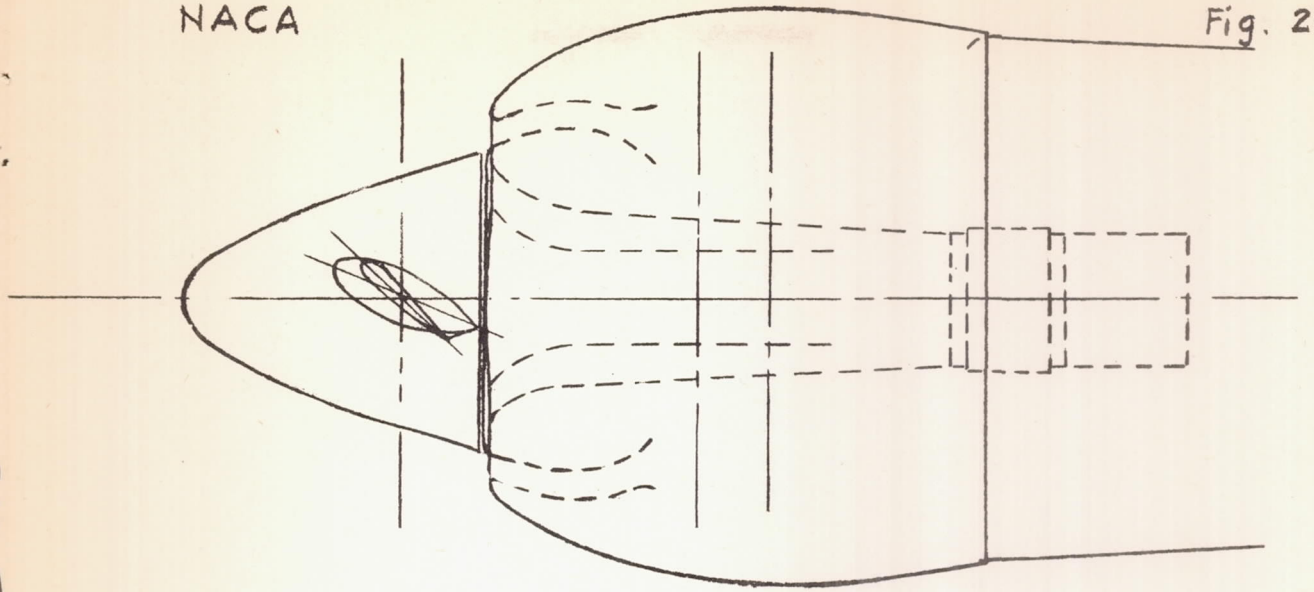

TOP VIEW

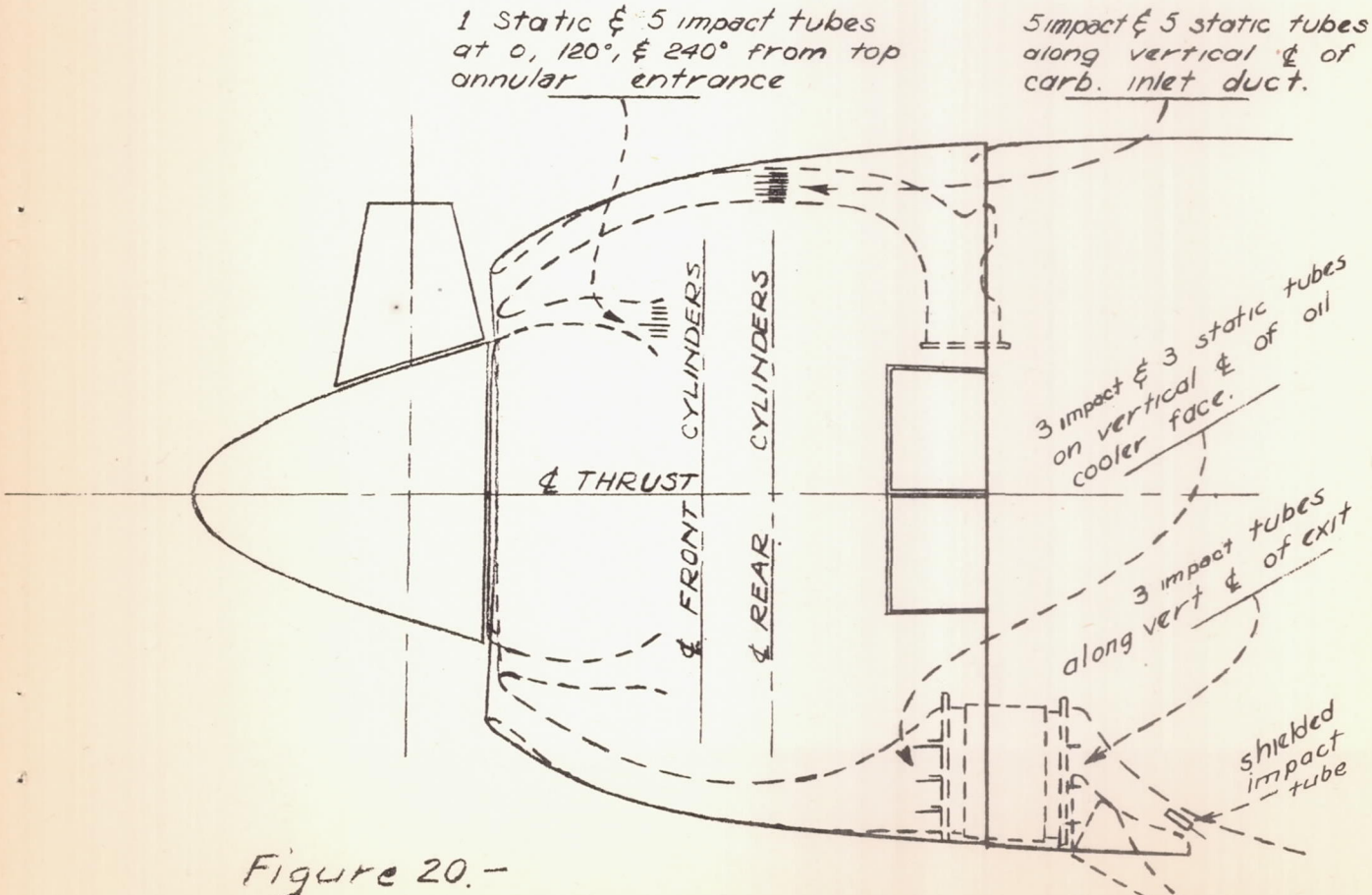

Figure 20.-
XP-42 SHORT-NOSE HIGH-INLET VELOCITY COWLING.

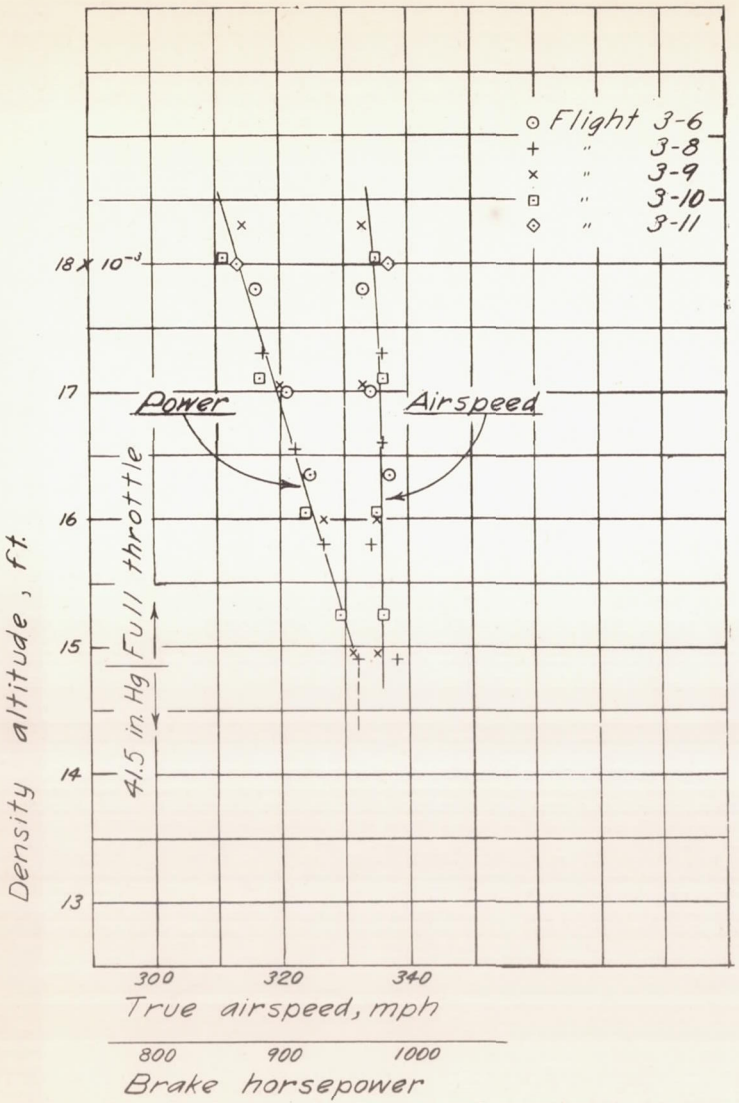

Figure 26.- Variation of airspeed and power with density altitude.

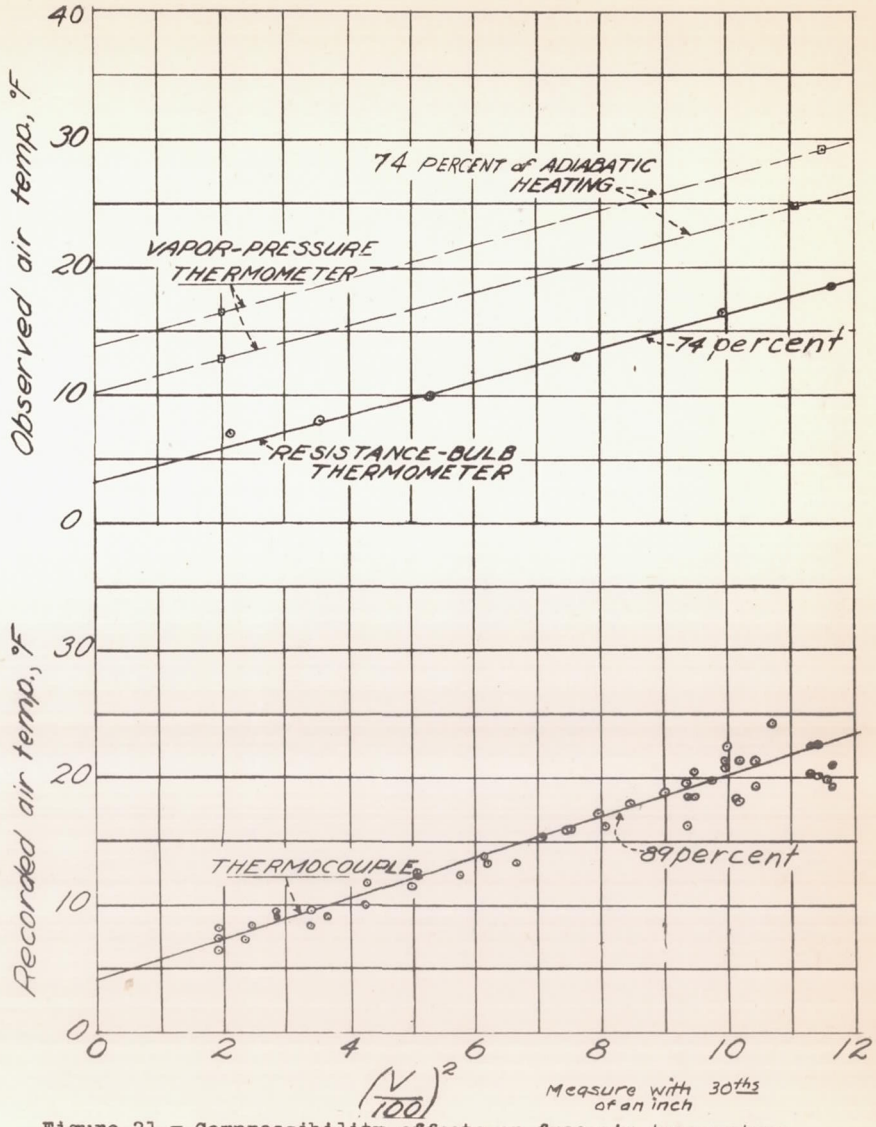

Figure 21.- Compressibility effects on free-air temperature measurements.

L-383

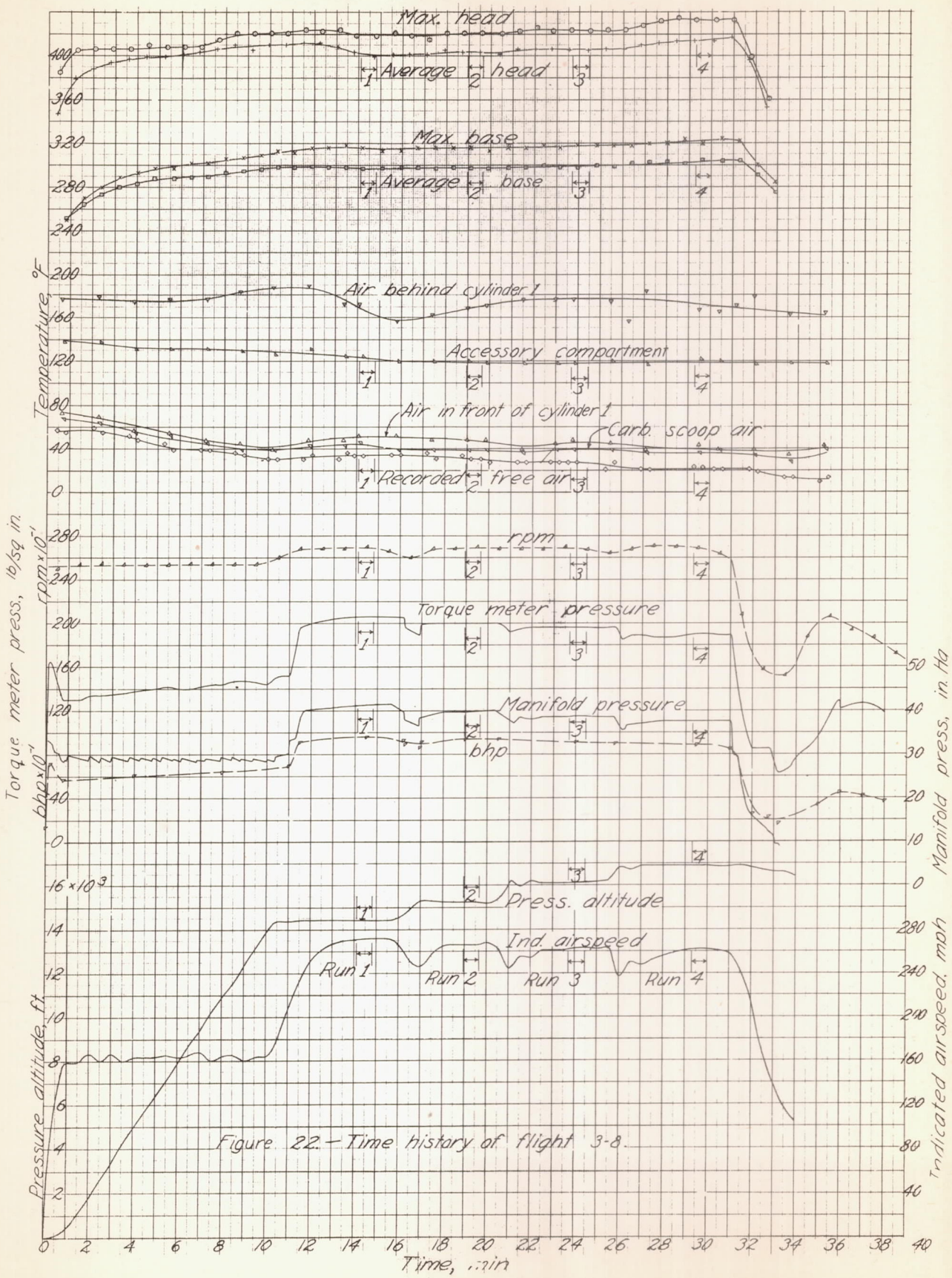

Figure 22.- Time history of flight 3-8.

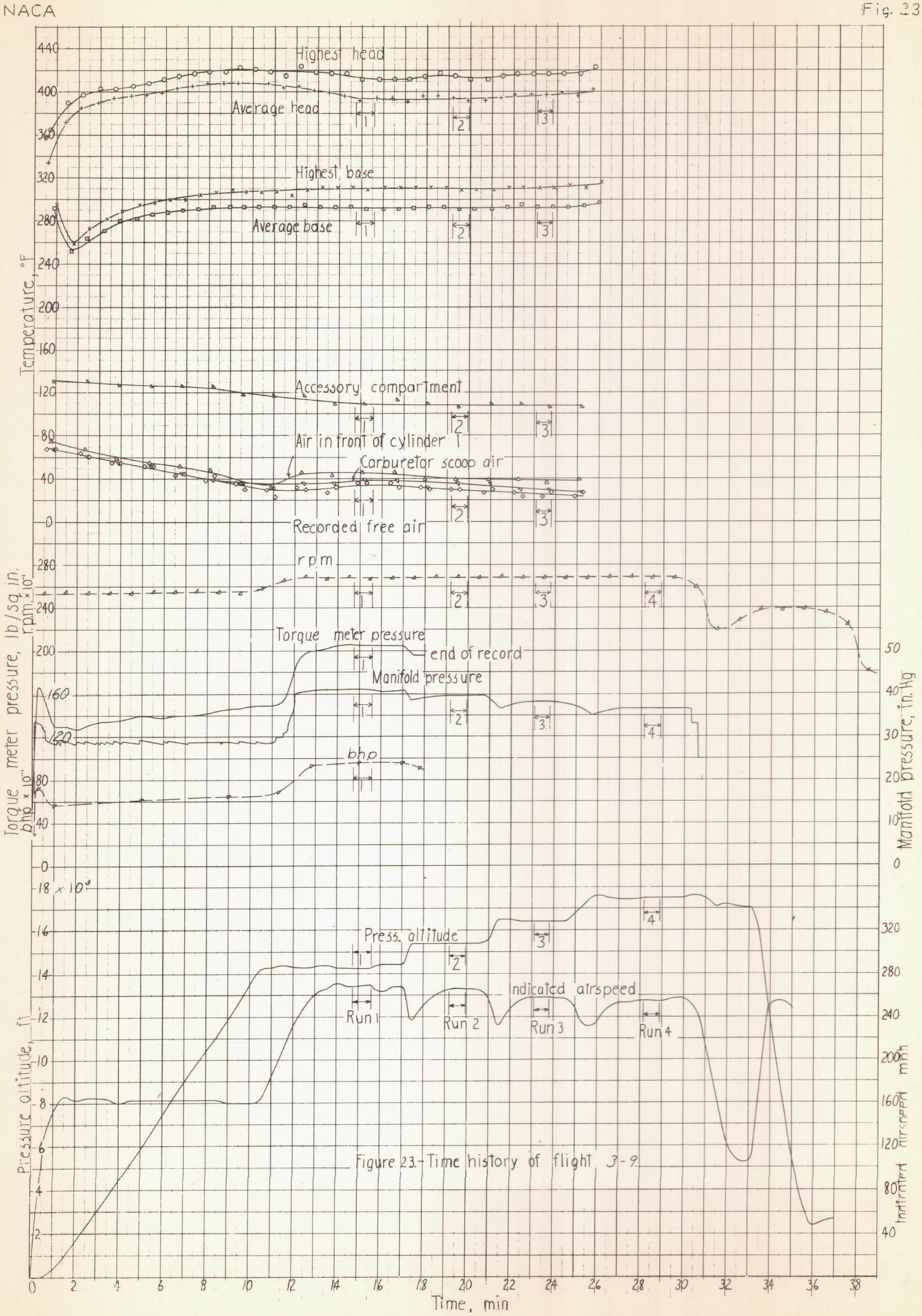

Figure 23.- Time history of flight 3-9.

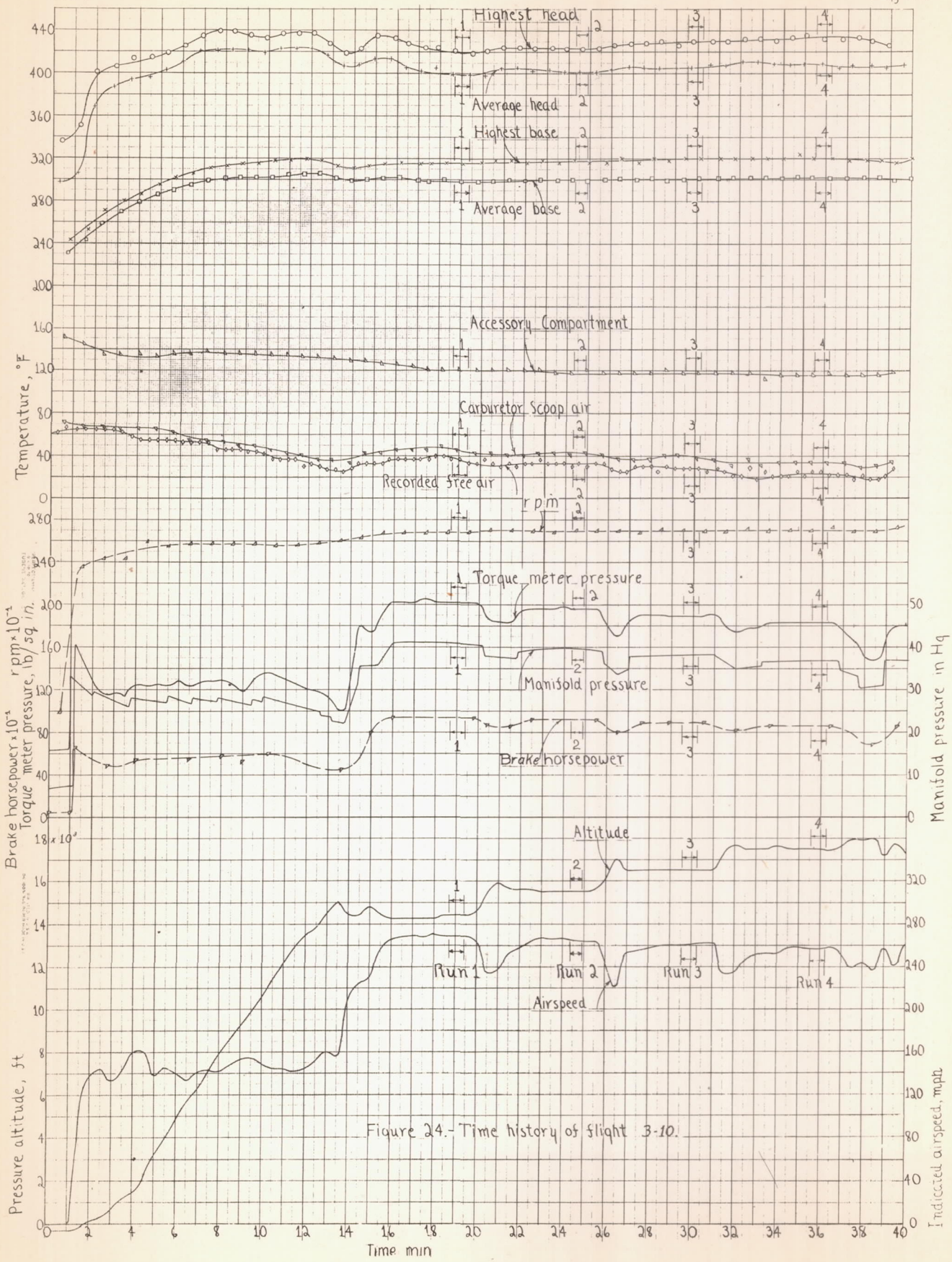

Figure 24.- Time history of flight 3-10.

L-383

L-383

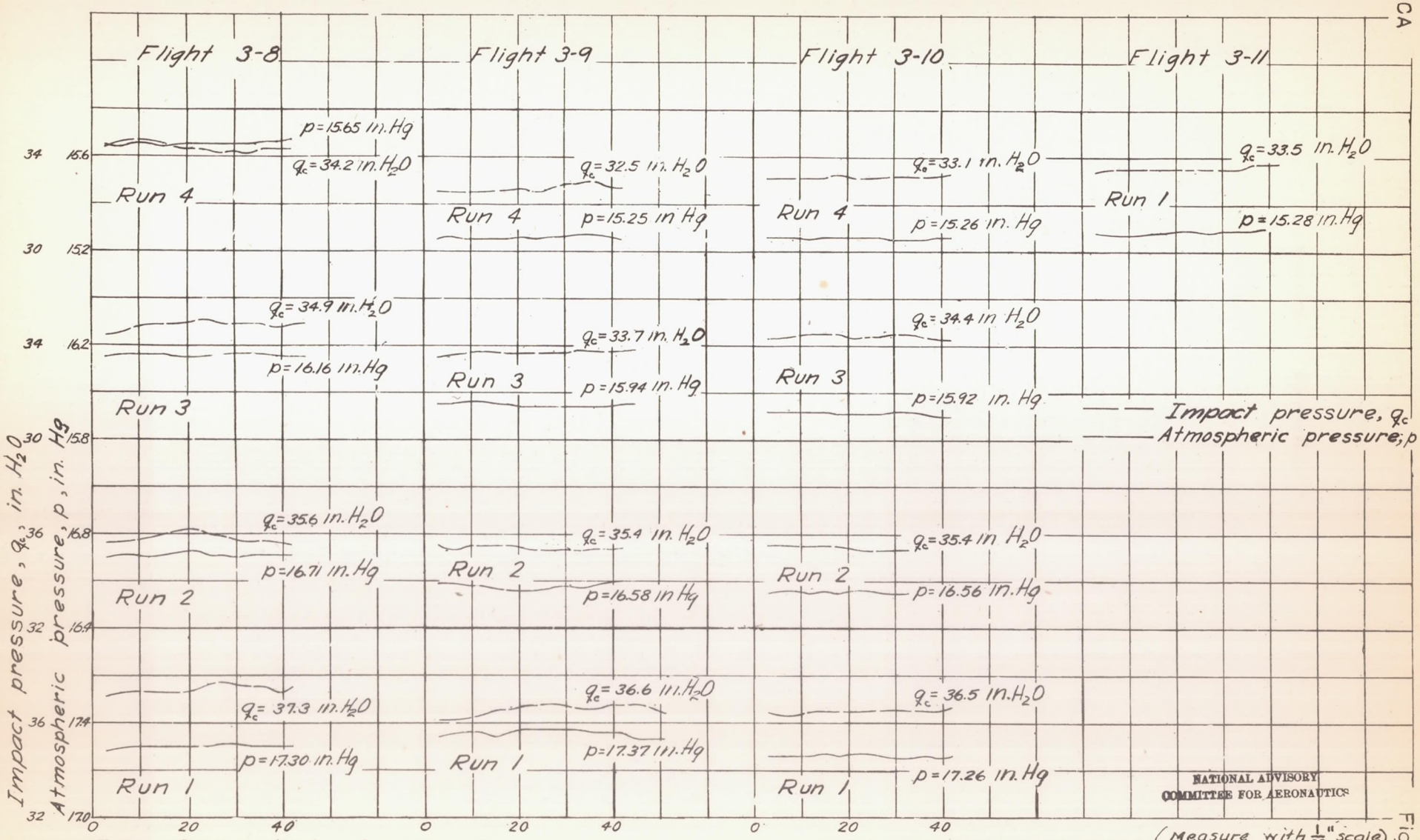

Figure 25.- Time histories of atmospheric and impact pressures during high-speed runs.

NACA Fig. 25

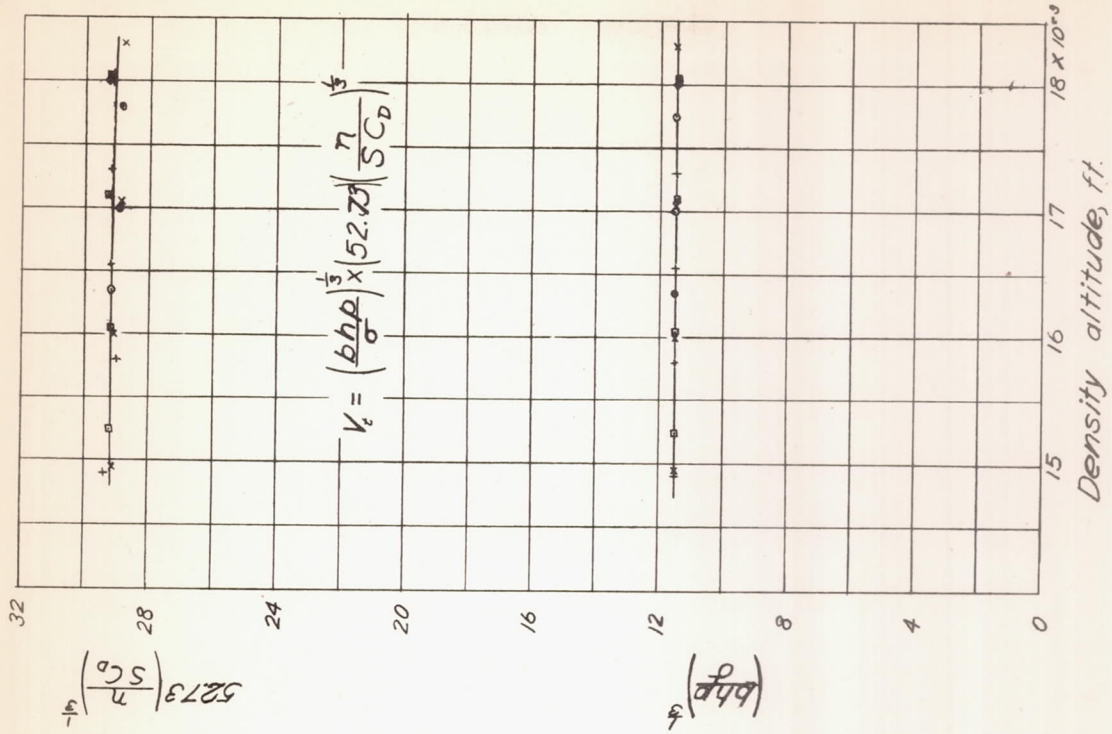

(Measure with 30ths of an inch)

Figure 27.- Analysis of high-speed performance.

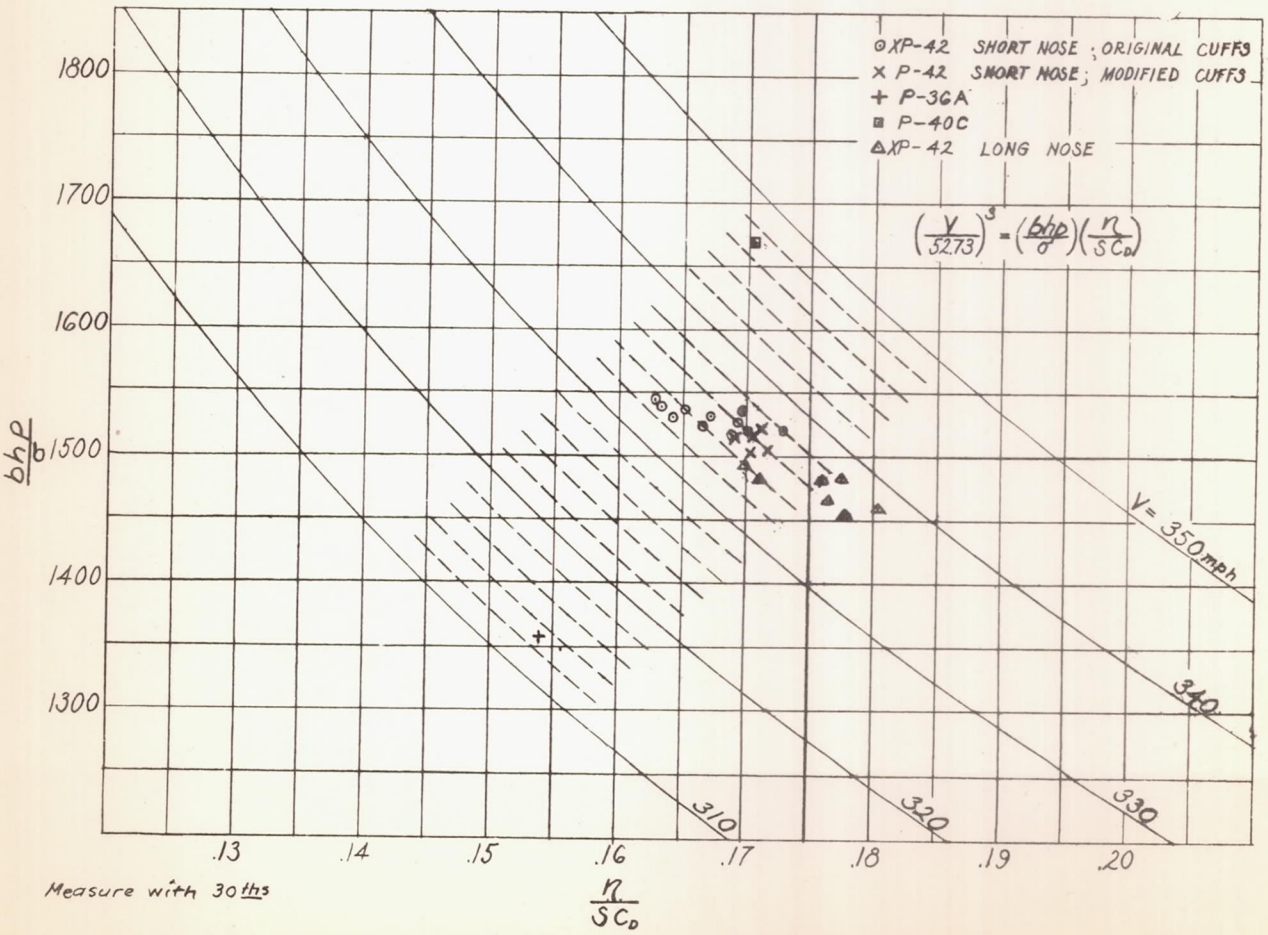

Figure 28.- Comparison of high-speed performance on several airplanes.

L-383

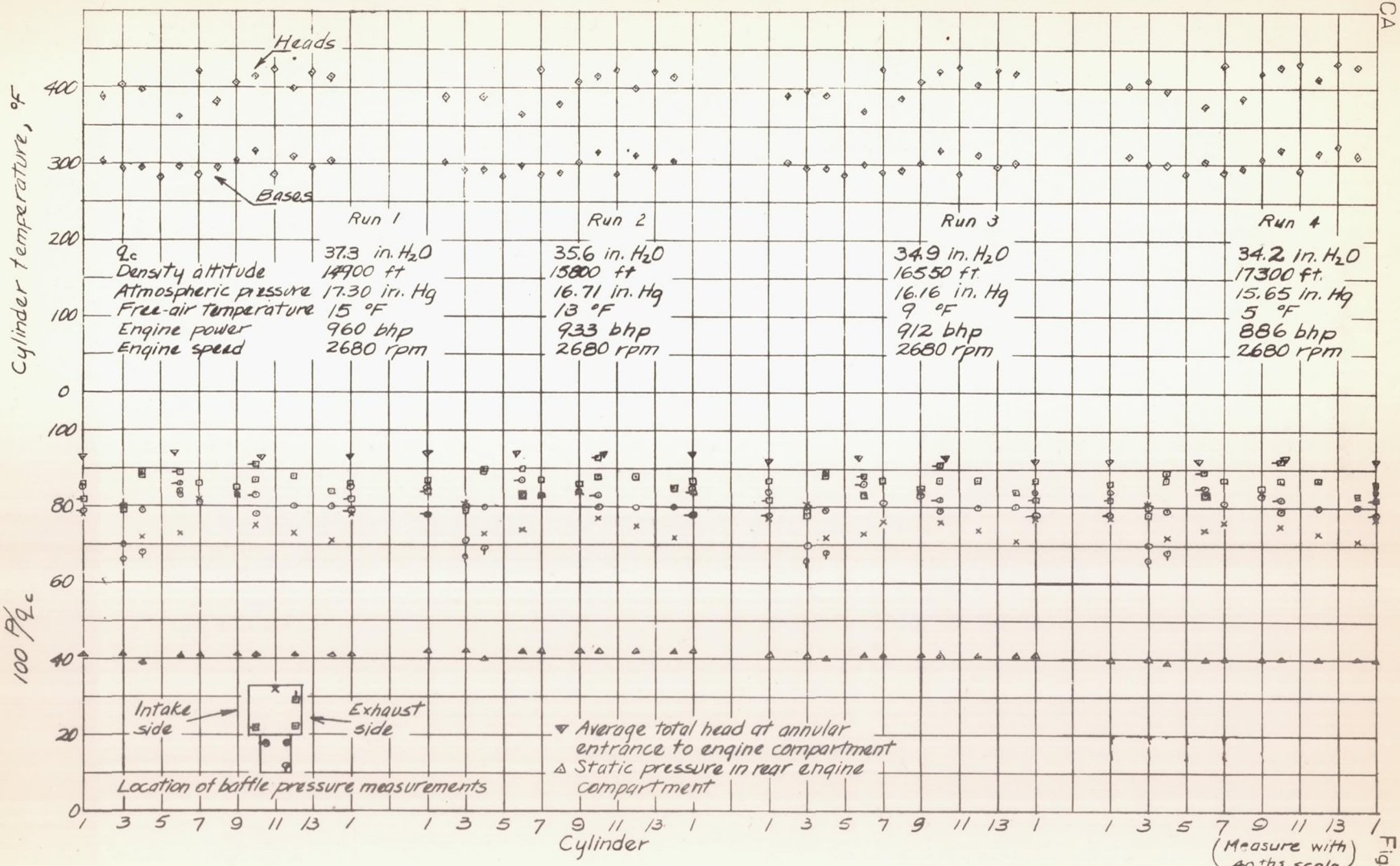

Figure 29.- Cooling-air pressure distribution and cylinder temperatures. Flight 3-8.

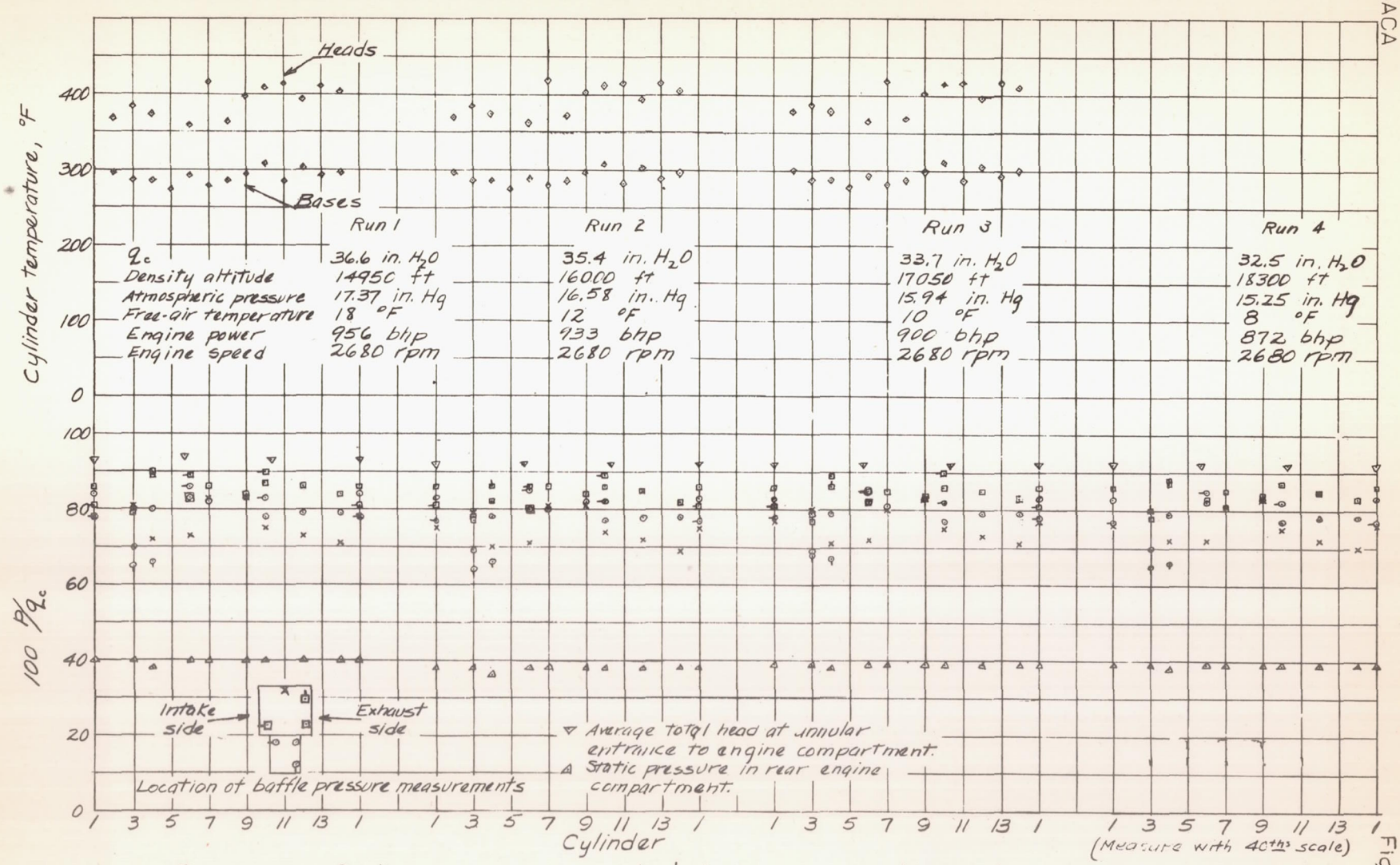

Figure 30.- Cooling-air pressure distribution and cylinder temperatures. Flight 3-9.

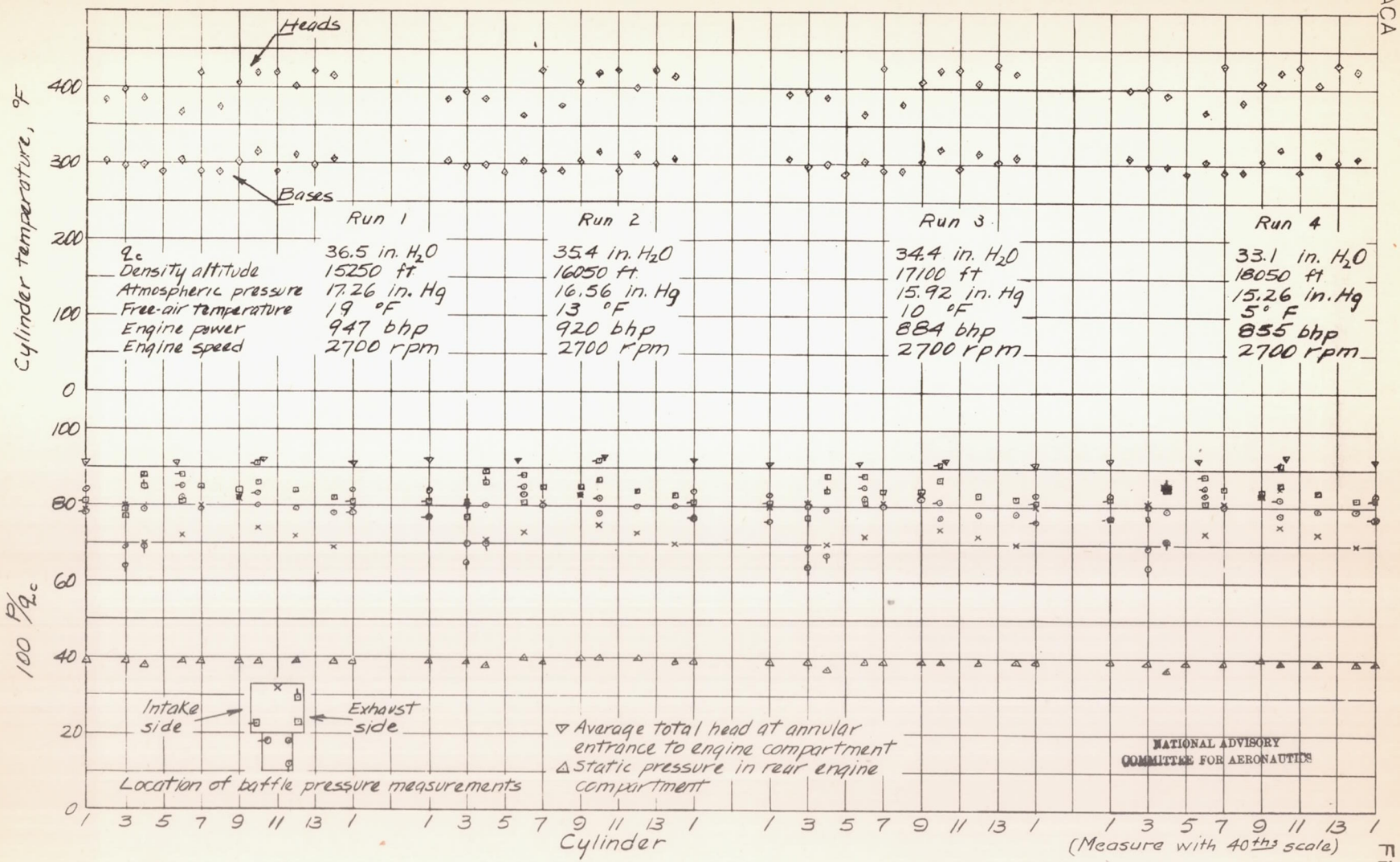

Figure 31.- Cooling-air pressure distribution and cylinder temperature. Flight 3-10.

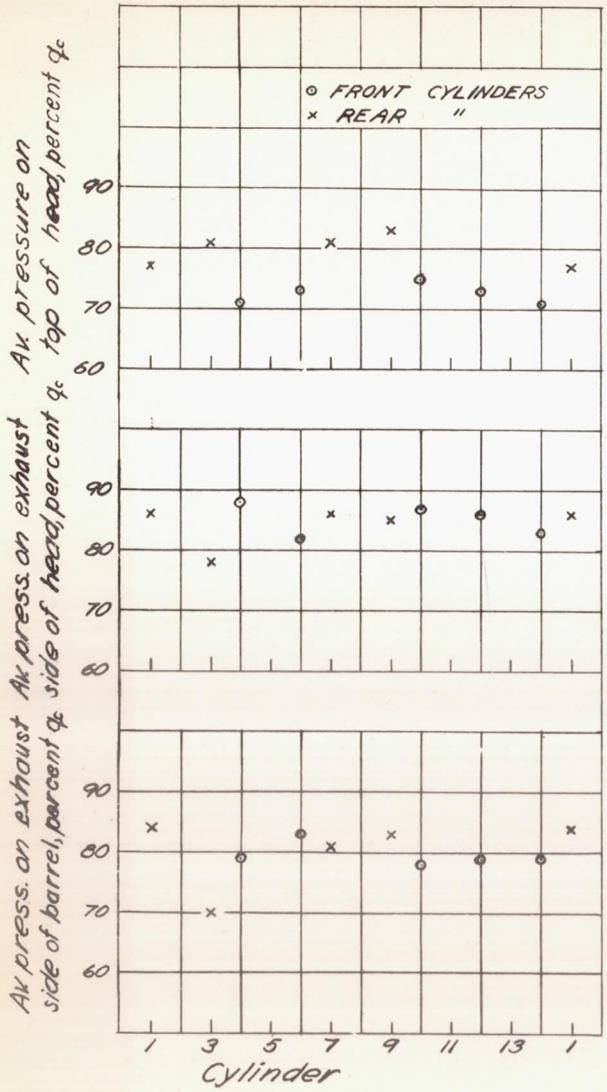

Figure 32.- Pressures at several locations on individual cylinders, averaged for all high-speed runs.

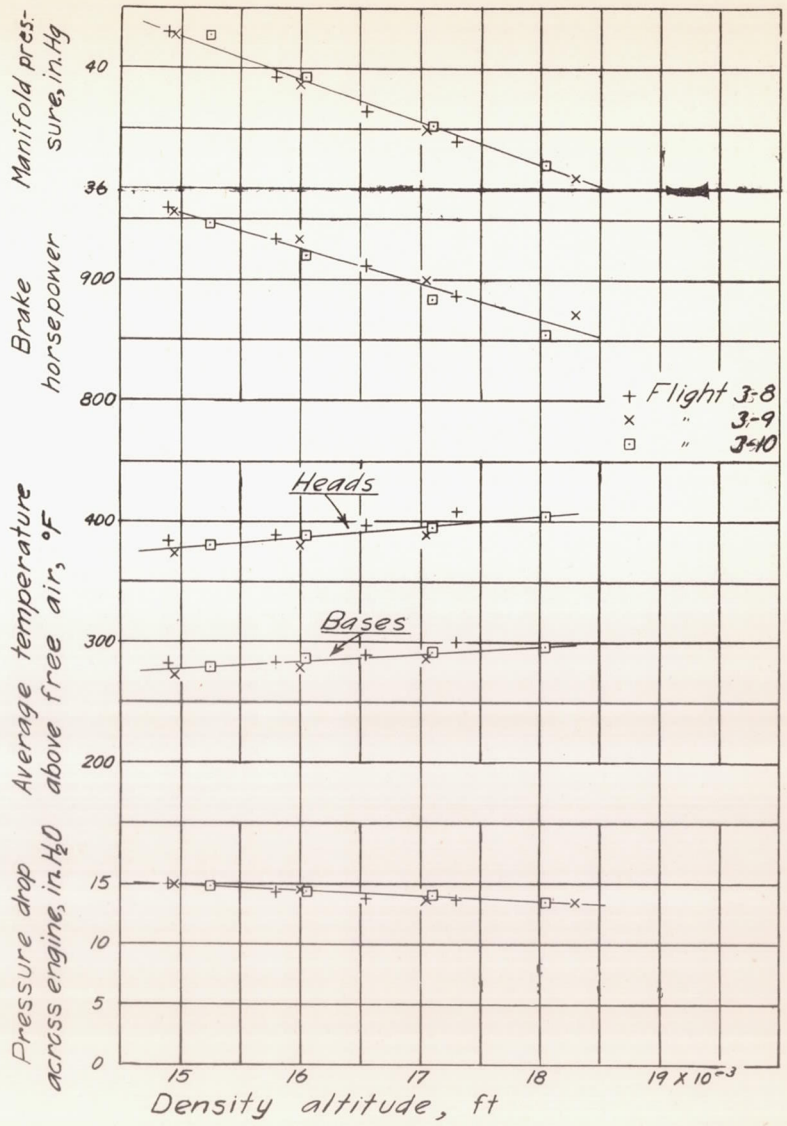

Figure 33.- Effect of altitude on cooling.

Measure with $\frac{5}{16}$" of inch

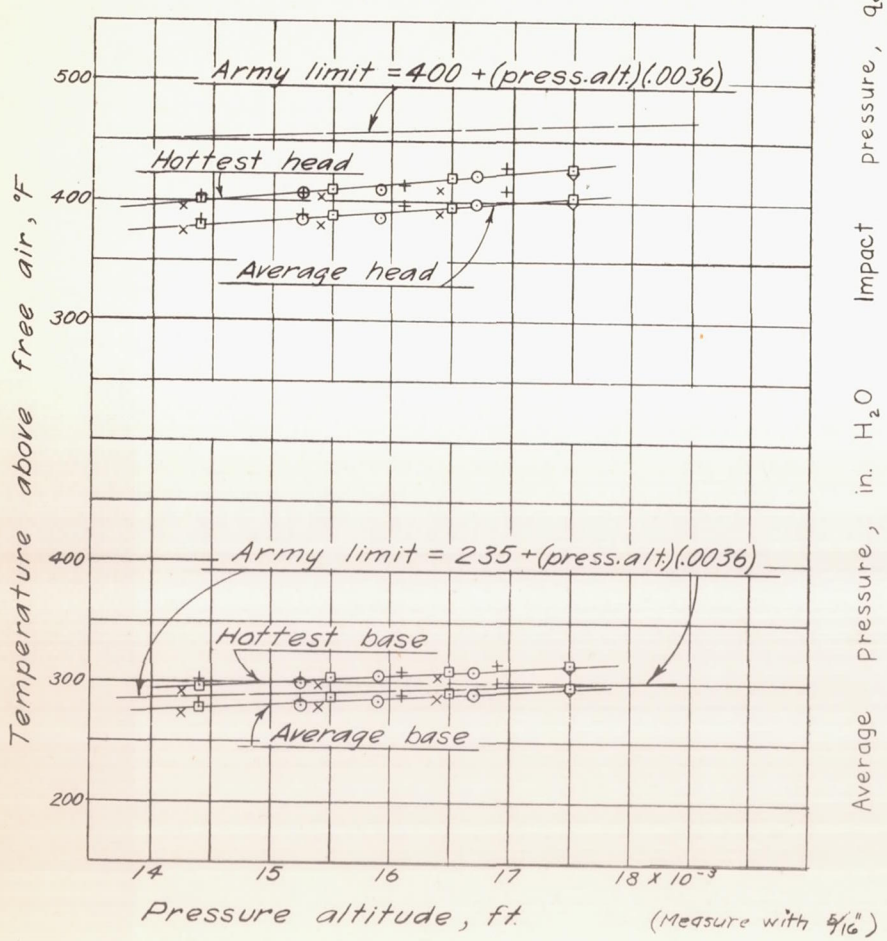

Figure 34.— Comparison of cylinder temperature with Army limits.

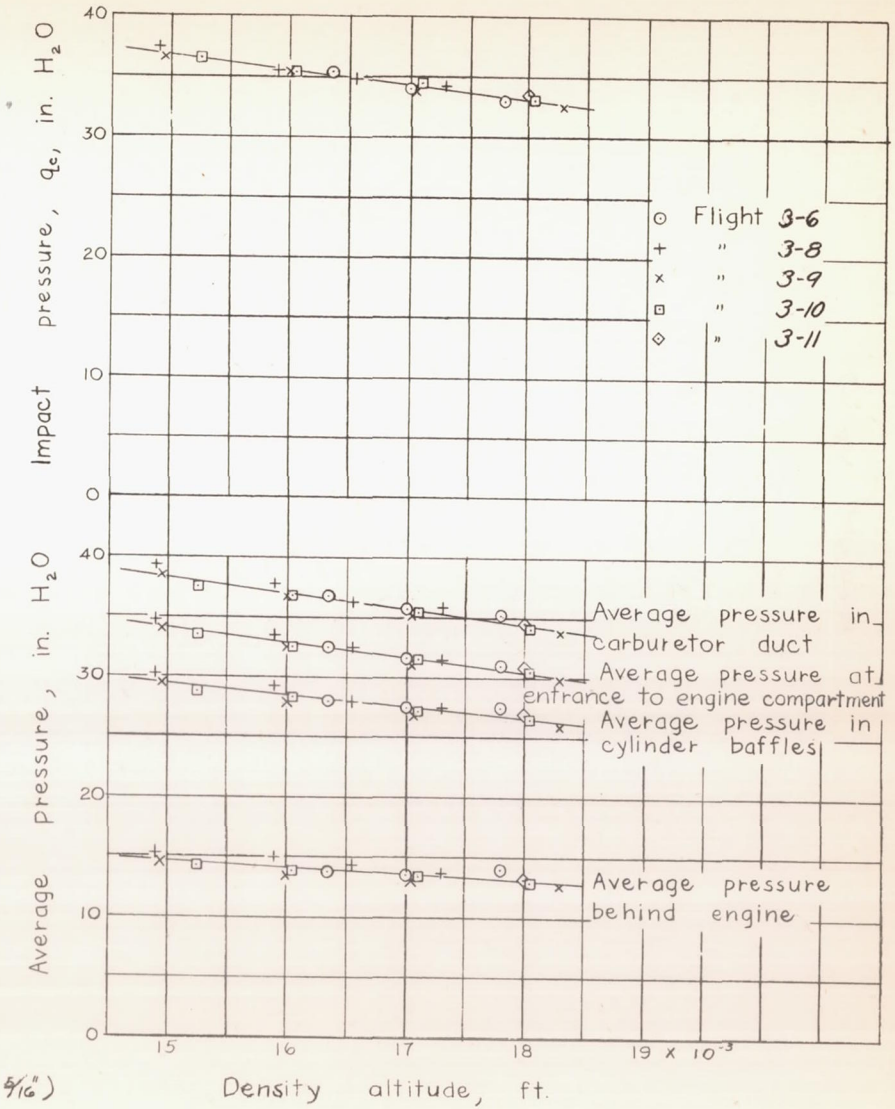

Figure 35.— Comparison of average induction and cooling-air pressures at several locations.

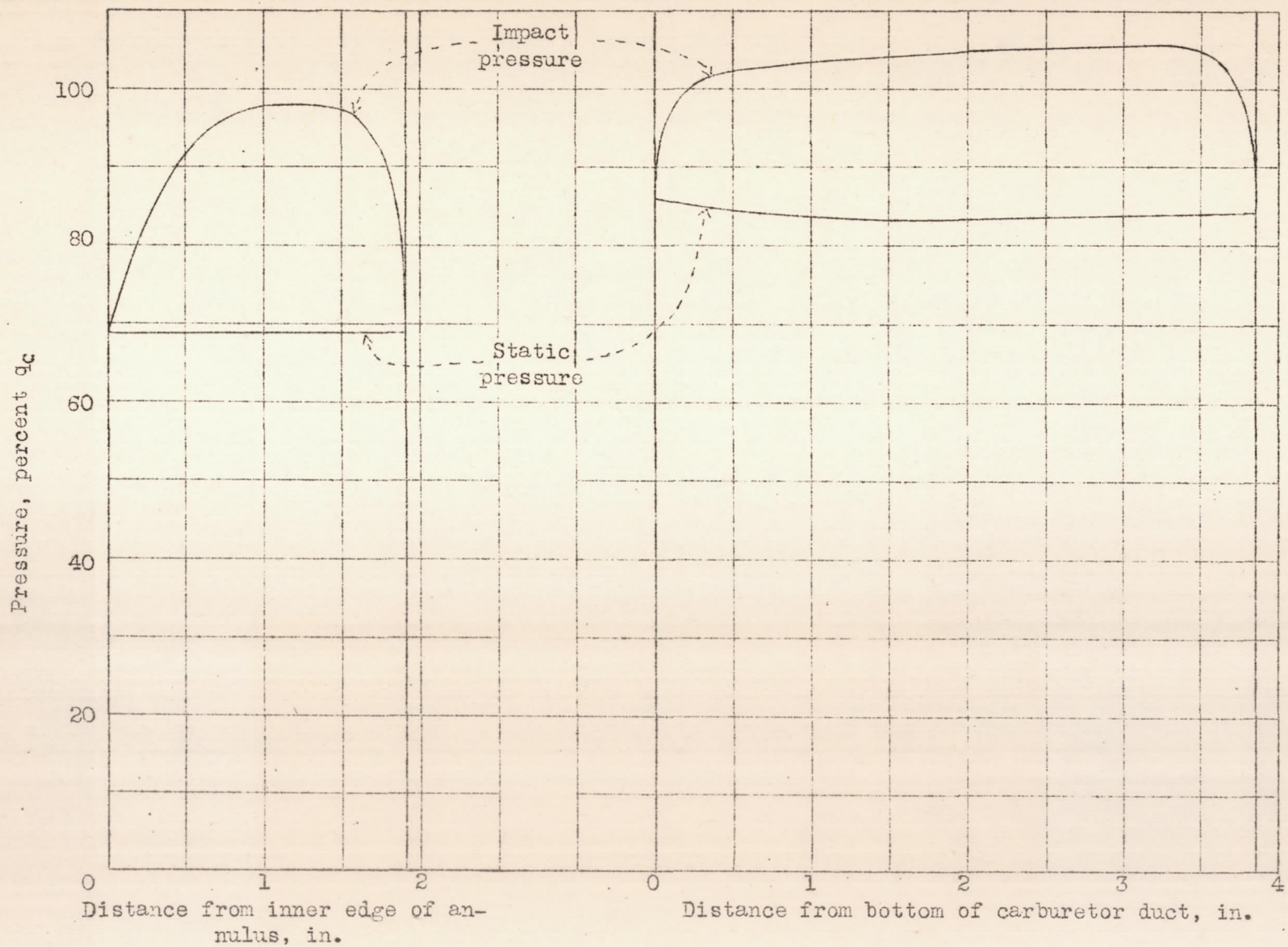

Figure 36.- Average pressure distribution in annular entrance to engine compartment and in carburetor duct.